NASA-CR-168304
19840006394

NASA Contractor Report 168304

FURTHER DEVELOPMENT OF A METHOD FOR COMPUTING THREE-DIMENSIONAL SUBSONIC VISCOUS FLOWS IN TURBOFAN LOBE MIXERS

Shyi-Jang Lin, J. P. Kreskovsky, W. R. Briley, and H. McDonald

Scientific Research Associates
Glastonbury, Connecticut

November 1983

Prepared for

NATIONAL AERONAUTICS AND SPACE ADMINISTRATION
Lewis Research Center
Under Contract NAS3-22758

LIST OF SYMBOLS

A	area
c_p	specific heat
C_{PT}	total pressure loss coefficient
$\mathcal{D}$	turbulent damping function
E	total enthalpy
F	viscous stress
G	viscous stress
h	metric coefficient
k	turbulent kinetic energy
ℓ	turbulent length scale
P	turbulence production
p	pressure
Q, q	magnitude of velocity vector
R	radius
R_ℓ, R_T	turbulent Reynolds numbers
T	temperature
u	velocity
v	radial velocity
w	azimuthal velocity
γ	ratio of specific heats
ε	turbulent dissipation
κ	von Karman's constant
μ	viscosity
ξ	vorticity
ρ	density
ϕ	scalar potential
ψ	stream function
Ω	vorticity

LIST OF SYMBOLS

Subscripts

I	inviscid
n	normal direction
p	primary
s	secondary
t	turbulent
v	viscous

TABLE OF CONTENTS

INTRODUCTION

Lobe mixers are devices which are currently being used for thrust augmentation on a variety of turbofan engines. The mixer is designed to provide a means of generating mixing between the turbine and fan streams before they enter the exhaust nozzle. Through careful design, the mixing can result in more uniform energy distribution at the nozzle exit. Provided that the losses incurred in the mixing process are minimized relative to the amount of mixing, small but significant performance gains may be realized.

Obviously, due to the sensitivity of mixer performance to changes in lobe shape and number, inlet velocity and temperature ratios, and secondary flows generated by the lobes, a computation procedure which could be used to sift through a matrix of possible design configurations would be of significant value. Such a procedure was previously developed by Kreskovsky, Briley and McDonald (Ref. 1), based on the velocity decomposition approach of Briley and McDonald (Ref. 2). The analysis synthesizes concepts from potential flow theory, secondary flow theory, and from an extension of three-dimensional boundary layer theory in a manner which allows efficient numerical solution by forward marching in space. The resulting procedure was used extensively in Refs. 3-5 to examine the effects of lobe shape, lobe generated secondary flows, and turbulence effects on mixing. The results obtained in Refs. 3-5 were, in general, found to be in excellent agreement with available experimental data.

Through interpretation of the results obtained using the analysis of Ref. 1, a more detailed understanding of the mixing processes in lobe mixers was obtained. As a result, it became apparent that it would be beneficial to extend the analysis of Ref. 1 and further develop and improve its capabilities. These extended capabilities, which are the subject of the present investigation, allow the current version of the analysis to be applied to mixer flows with swirl, and to allow more general specification of initial condition with nonzero secondary flow vorticity. In addition, the procedure for determining the required a priori compressible potential flow pressure gradients from an incompressible flow solution, has been improved. Finally, the formulation of the κ-ε turbulence model used in the previous version of the procedure was somewhat unreliable, leading in some instances to predictions of negative values of turbulence kinetic energy. Under the current investigation, the reliability of this model was improved by making minor changes in the numerical formulation, and optional turbulence models were added to the procedure.

As a result, the present version of the mixer analysis and computer code represents a reliable, improved analysis with extended capabilities which can be used to further the understanding of lobe mixer flow fields, and to aid in mixer design.

ANALYSIS

General Approach

The present analysis is described in detail in Ref. 1, and is outlined only briefly here. The analysis is based on approximations made relative to a curvilinear but not necessarily orthogonal coordinate system fitted to and aligned with the flow geometry under consideration (cf. Fig. 1). The coordinate system is chosen such that the streamwise or marching coordinate downstream of the lobes either coincides with or is at least approximately aligned with a known inviscid primary flow direction, as determined for example by a potential flow for the given geometry. Transverse coordinate surfaces must be either perpendicular or nearly perpendicular to solid walls or bounding surfaces, since diffusion is permitted only in these transverse coordinate surfaces.

Equations governing streamwise vorticity and a scalar viscous correction u_v to a known inviscid primary flow velocity $\bar{U}_I$ are derived utilizing assumptions which permit forward-marching solution, provided reversal of the composite streamwise velocity does not occur. Terms representing diffusion normal to transverse coordinate surfaces are neglected. Approximate pressure gradients are derived from the inviscid primary flow and imposed in the streamwise momentum equation. Secondary flow velocities are determined by scalar and vector potentials in the transverse coordinate surfaces, to suppress streamwise elliptic behavior requiring downstream boundary conditions. Finally, the use of streamwise vorticity in obtaining secondary flow velocities avoids the explicit use of transverse momentum equations in predicting the secondary flow velocities.

Primary-Secondary Velocity Decomposition

The analysis is based on decomposition of the overall velocity vector field $\bar{U}$ into a primary flow velocity $\bar{U}_p$ and a secondary flow velocity $\bar{U}_s$. The overall or composite velocity is determined from the super-position

$$\bar{U} = \bar{U}_p + \bar{U}_s \tag{2.1}$$

For lobe mixer flows the primary flow velocity is represented as

$$\bar{U}_p = \bar{U}_I u_v \tag{2.2}$$

where $\bar{U}_I$ is a known inviscid primary flow velocity satisfying slip conditions and determined from an <u>a priori</u> potential flow solution in the geometry under

consideration. The (non-dimensional) scalar quantity u_v is a viscous velocity profile factor which introduces viscous shear layers and may also correct for internal flow blockage effects. In the present case of the lobe mixer u_v accounts for both boundary layers and the free shear layer which exists between the fan and turbine streams. The viscous velocity correction u_v is determined from solution of a primary flow momentum equation. As will become apparent, for the lobe mixer it is conventient to solve for the component of $\bar{U}_p$ in the primary flow direction rather than u_v.

To suppress streamwise elliptic behavior, the secondary flow velocity $\bar{U}_s$ is defined by, and presumed derivable from, scalar and vector surface potentials denoted ϕ and ψ, respectively. If $\hat{i}_1$ denotes the unit vector normal to transverse coordinate surfaces (also presumed here to be in the direction of the marching coordinate), if ρ is density, and if ρ_o is an arbitrary constant reference density, then $\bar{U}_s$ is defined by

$$\bar{U}_s \equiv \nabla_s\phi + (\rho_o/\rho)\nabla\times\hat{i}_1\psi \tag{2.3}$$

where ∇_s is the surface gradient operator defined by

$$\nabla_s \equiv \nabla - \hat{i}_1(\hat{i}_1\cdot\nabla) \tag{2.4}$$

It follows that $\hat{i}_1 \cdot \bar{U}_s = 0$ and thus $\bar{U}_s$ lies entirely within transverse coordinate surfaces. Equation (2.3) is a general form permitting both rotational and irrotational secondary flows and will lead to governing equations which are elliptic in transverse coordinate surfaces and which are, therefore, solvable within a forward-marching context. The overall velocity decomposition (2.1) can be written

$$\begin{aligned}\bar{U} &= \bar{U}_I u_v + \nabla_s\phi + (\rho_o/\rho)\nabla\times\hat{i}_1\psi \\ &= \bar{u}_p + \nabla_s\phi + (\rho_o/\rho)\nabla\times\hat{i}_1\psi\end{aligned} \tag{2.5}$$

Surface Potential Equations

Equations relating ϕ and ψ with u_v, ρ, and the streamwise vorticity component Ω_1 can be derived from Eq. (2.5) as follows:

$$\nabla\cdot\rho\bar{U} = 0 = \nabla\cdot\rho\bar{U}_I u_v + \nabla\cdot\rho\nabla_s\phi + \rho_o\nabla\cdot\nabla\times\hat{i}_1\psi \tag{2.6}$$

$$\hat{i}_1\cdot\nabla\times\bar{U} \equiv \Omega_1 = \hat{i}_1\cdot\nabla\times\bar{U}_I u_v + \hat{i}\cdot\nabla\times(\rho_o/\rho)\nabla\times\hat{i}_1\psi + \hat{i}_1\cdot\nabla\times\nabla_s\phi \tag{2.7}$$

Since the last term in each of Eqs. (2.6, 2.7) is zero by vector identity, Eqs. (2.6, 2.7) can be written as

$$\nabla\cdot\rho\nabla_s\phi = -\nabla\cdot\rho\bar{U}_I u_v \tag{2.8}$$

$$\hat{i}_1\cdot\nabla\times(\rho_o/\rho)\nabla\times\hat{i}_1\psi = \Omega_1 - \hat{i}_1\cdot\nabla\times\bar{U}_I u_v \tag{2.9}$$

which are elliptic for ϕ and ψ in transverse coordinate surfaces. The last term in Eq. (2.9) is identically zero in a potential flow coordinate system for which $\hat{i}_1$ and $\bar{U}_I$ have the same direction, and is small if $\hat{i}_1$ and $\bar{U}_I$ are approximately aligned. Given a knowledge of u_v, Ω, and ρ, the surface potentials ϕ and ψ can be determined by a two-dimensional elliptic calculation in transverse coordinate surfaces at each streamwise location. In turn, $\bar{U}_s$ can be computed from Eq. (2.3), and the composite velocity $\bar{U}$ will satisfy continuity. Equations for u_v and Ω_1 are obtained from the equations governing momentum and vorticity, respectively.

Primary Momentum and Pressure Approximation

The streamwise momentum equation is given by

$$\hat{i}_1\cdot\left[(\bar{U}\cdot\nabla)\bar{U} + (\nabla p)/\rho\right] = \hat{i}_1\cdot\bar{F} \tag{2.10}$$

where p is pressure and $\rho\bar{F}$ is force due to viscous stress. Terms in F representing streamwise diffusion are neglected; however, since the viscous terms are complex for compressible flow, the modified viscous force is temporarily denoted $\bar{F}'$, and further consideration of viscous terms is deferred to a later section.

The remaining assumption for Eq. (2.10) concerns the pressure gradient term and is designed to permit numerical solution as an initial value problem. An obvious pressure approximation for curved flow geometries is to impose pressure gradients from an inviscid potential flow (Briley [6]), and for internal flows, to correct these with a mean pressure gradient term depending only on the x_1 coordinate (Pantankar & Spalding [7]). This approximation is appropriate both for flows consisting of an irrotational core region with thin shear layers on bounding surfaces, and also for some fully viscous flows.

If pressure gradients are derived from the inviscid potential velocity $\bar{U}_I$, and if a mean viscous pressure correction $p_v(x_1)$ is introduced, the pressure approximation can be written as

$$\hat{i}_1 \cdot \nabla p + \hat{i}_1 \cdot \left[\nabla p_v(x_1) - \rho \nabla (\bar{U}_I \cdot \bar{U}_I)/2 \right] \equiv \hat{i}_1 \cdot \nabla (p_I + p_v) \tag{2.11}$$

where p_I is the imposed pressure. Typically, for internal flows, p_v is determined to ensure that an integral mass flux condition is satisfied, such as

$$\int_A \hat{i}_1 \cdot \rho \bar{U} \, dA = \text{constant} \tag{2.12}$$

Combining Eqs. (2.10) and (2.11) and setting $\bar{F} \doteq \bar{F}'$ provides an equation nominally governing u_v:

$$\hat{i}_1 \cdot \left[(\bar{U} \cdot \nabla)\bar{U} + (\nabla p_v)/\rho - \nabla (\bar{U}_I \cdot \bar{U}_I)/2 \right] = \hat{i}_1 \cdot \bar{F}' \tag{2.13}$$

where $\bar{U}$ is to be written as

$$\bar{U} = \hat{i}_1 u_I u_v + \hat{i}_2 (v_I u_v + v_s) + \hat{i}_3 (w_I u_v + w_s) \tag{2.14}$$

where u_I, v_I, w_I are components of $\bar{U}_I$, and v_s, w_s are components of $\bar{U}_s$.

Secondary Vorticity

An equation governing Ω_1 in compressible flow can be obtained from an approximate application of secondary flow theory. The equation governing the growth of vorticity Ω_s along a streamline for compressible flow with constant viscosity is given by Lakshminarayana & Horlock [8] and may be written for variable viscosity as

$$\frac{\partial}{\partial s}\left(\frac{\Omega_s}{\rho q}\right) = \frac{2\Omega_n}{\rho q R} - \frac{1}{\rho q^2} \hat{s} \cdot \nabla \times \frac{1}{\rho} \nabla p + \frac{1}{\rho q^2} \hat{s} \cdot \bar{G} \tag{2.15}$$

where q is velocity magnitude, $\hat{s}$ is the unit vector along a streamline, s is distance along a streamline, Ω_n is vorticity in the direction of the unit principal normal vector $\hat{n}$ of the streamline, for which R is the principal radius of curvature. These quantities are related by the Frenet formula

$\hat{n}/R = \partial\hat{s}/\partial s = \hat{s} \cdot \nabla\hat{s}$. In Eq. (2.15), $\bar{G} \equiv \nabla \times \bar{F}$, and the term containing p vanishes if ρ is constant. Since an intrinsic coordinate system formulation as in Eq. (2.15) provides an "inverse" coordinate system if used to compute $\bar{U}$, and since intrinsic coordinates are degenerate on no-slip surfaces and nonorthogonal for general rotational flows, intrinsic coordinates are not attractive for numerical computation. However, if the coordinate system used for computation is approximately aligned with the flow direction, then an approximate equation governing Ω_s can be derived from Eq. (2.15) by replacing $\hat{s}$ by $\hat{i}$, as in the following development:

$$\frac{\Omega_s}{q} = \frac{\hat{s}\cdot\bar{\Omega}}{\hat{s}\cdot\bar{U}} \doteq \frac{\hat{i}_1\cdot\bar{\Omega}}{\hat{i}_1\cdot\bar{U}} = \frac{\Omega_1}{u_1} \tag{2.16a}$$

$$\frac{\Omega_n}{qR} = \frac{(\hat{s}\cdot\nabla\hat{s})\cdot\bar{\Omega}}{\hat{s}\cdot\bar{U}} \doteq \frac{(\hat{i}_1\cdot\nabla\hat{i}_1)\cdot\bar{\Omega}}{\hat{i}_1\cdot\bar{U}} = \frac{\Omega_{n1}}{u_1 R_1} \tag{2.16b}$$

where $u_1 = u_I u_v$; R_1 is the principal radius of curvature of the x_1 coordinate, and Ω_{n1} is vorticity in the direction of $\hat{n}_1$, the principal normal of the x_1 coordinate line. The quantities $\hat{n}_1$ and R_1 are defined by the Frenet formula $\hat{n}_1/R_1 = \hat{i}_1 \cdot \nabla\hat{i}_1$. To illustrate, in an orthogonal coordinate system,

$$\frac{\hat{n}_1}{R_1} = -\left[\frac{\hat{i}_2}{h_1 h_2}\frac{\partial h_1}{\partial x_2} + \frac{\hat{i}_3}{h_1 h_3}\frac{\partial h_1}{\partial x_3}\right] \tag{2.17}$$

where h_1, h_2, h_3 denote metric coefficients. If ρ varies, p is replaced by the imposed pressure p_I as defined in Eq. (2.11). Finally, taking $q^2 \doteq u_1^2$ and $\hat{s} \doteq \hat{i}_1$ in the last two terms in Eq. (2.15), and neglecting streamwise diffusion, Eq. (2.15) becomes

$$\bar{U}\cdot\nabla\left(\frac{\Omega_1}{\rho u_1}\right) = \frac{2\Omega_{n1}}{\rho u_1 R_1} - \frac{1}{\rho u_1^2}\hat{i}_1\cdot\nabla\times\left(\frac{\nabla p_I}{\rho}\right) + \frac{1}{\rho u_1^2}\hat{i}_1\cdot\bar{G}' \tag{2.18}$$

where $\bar{G}'$ does not contain streamwise diffusion.

The transverse vorticity Ω_{ni} in Eq. (2.18) contains components which, in orthogonal coordinates and assuming an irrotational $\bar{U}_I$, are given by

$$\Omega_2 = \hat{i}_2 \cdot \nabla \times \bar{U} = \frac{u_I}{h_3}\frac{\partial u_v}{\partial x_3} - \frac{w_I}{h_1}\frac{\partial u_v}{\partial x_1} - \frac{1}{h_1 h_3}\frac{\partial}{\partial x_1}(h_3 w_s) \tag{2.19a}$$

$$\Omega_3 = \hat{i}_3 \cdot \nabla \times \bar{U} = -\frac{u_I}{h_2}\frac{\partial u_v}{\partial x_2} + \frac{v_I}{h_1}\frac{\partial u_v}{\partial x_1} + \frac{1}{h_1 h_2}\frac{\partial}{\partial x_1}(h_3 v_s) \tag{2.19b}$$

In the applications contemplated here, the first term on the right-hand side of each of Eqs. (2.19a-b) is expected to dominate, and the remaining terms may be neglected as a convenience.

Energy Equation

Since the flow being considered is nonadiabatic, solution of an equation governing energy is required. The energy equation can be written in a variety of forms, one of which is

$$\rho \bar{U} \cdot \nabla E = \nabla \cdot k \nabla T + \bar{U} \cdot \bar{F} + \Phi \tag{2.20}$$

where E is total enthalpy, T is temperature, k is thermal conductivity, and Φ is the dissipation function. Solution of Eq. (2.20) by forward marching integration requires only that terms representing streamwise conduction of heat and also streamwise viscous diffusion in $\bar{F}$ be neglected.

Compressibility Relations

In the imposition of streamwise pressure gradients, compressibility effects are represented by introducing the perfect gas equation of state $p = \rho RT$. No other assumptions are necessary for consideration of compressible flow. For moderate subsonic Mach numbers, inviscid pressure gradients would ideally be obtained from a compressible potential flow calculation or otherwise from an incompressible potential flow corrected for compressibility using a suitable compressibility correction. Replacing p in Eq. (2.11) by the state equation and eliminating temperature using the temperature-enthalpy relation

$$E = c_p T + \frac{\bar{U} \cdot \bar{U}}{2} \tag{2.21}$$

where c_p denotes specific heat, the following auxiliary equation relating the imposed pressure gradients with density, velocity, and total enthalpy is obtained:

$$\hat{i}_1 \cdot \nabla\left[p_I + p_v(x_1)\right] = \hat{i}_1 \cdot \nabla\left[\frac{\gamma-1}{\gamma}\rho\left(E - \frac{\bar{U}\cdot\bar{U}}{2}\right)\right] \tag{2.22}$$

where γ is specific heat ratio. A slight simplification results if $\bar{U} \cdot \bar{U}$ is replaced by $(\hat{i}_1 \cdot \bar{U})^2$ in Eq. (2.22).

Governing System of Equations

A complete system of six coupled equations governing u_v, Ω_1, ϕ, ψ, E, and ρ is given by Eqs. (2.8), (2.9), (2.13), (2.20), (2.22), and (2.18). Ancillary relations are given by Eq. (2.5) for composite velocity, Eq. (2.12) for mass flux, and Eqs. (2.19a-b) for transverse vorticity.

The Turbulence Models

The present analysis is to be used to predict a turbulent flow field, thus the stress terms F' and G' in Eqs. (2.13), (2.18), and (2.20) contain turbulent shear terms in the form of fluctuating velocity and velocity-temperature correlations. These terms may be modeled using any one of a number of turbulence models which have been included in the present analysis. In general these turbulent shear terms are modeled through the introduction of a turbulent eddy viscosity, and this eddy viscosity may be computed from one of three optional turbulence models. The most complex and general turbulence model used in the present analysis is the κ-ε turbulence model described by Launder and Spalding (Ref. 9).

The transport equations governing k and ε are given in vector form (Ref. 9) for steady flow as

$$\rho U \cdot \nabla k = \nabla\left(\mu + \mu_T/\sigma_k\right)\nabla k + P - \rho\epsilon \tag{2.23}$$

$$\rho U \cdot \nabla \epsilon = \nabla \cdot \left(\mu + \mu_T/\sigma_\epsilon\right)\nabla k + C_1\frac{\epsilon}{k}P - C_2\frac{\rho\epsilon^2}{k} \tag{2.24}$$

In Eqs. (2.23, 2.24), P is the turbulence production. The quantities σ_k, σ_ε, C_1, C_2 are empirical constants which, as recommended by Launder & Spalding (Ref. 9), are taken as 1.0, 1.3, 1.44, and 1.92, respectively. Upon solution

of Eqs. (2.23 and 2.24) the turbulent viscosity and length scale may be computed as

$$\mu_T = C_\mu \rho k^2/\epsilon \tag{2.25}$$

and

$$\ell = C_\mu^{1/4} k^{3/2}/\epsilon \tag{2.26}$$

If low Reynolds number flows are considered (i.e. wall boundary layers are resolved) the constants C_μ and C_2 are adjusted from their high Reynolds number values. As suggested by Launder and Spalding (Ref. 9), C_2 is given as

$$C_2 = C_{2\infty}(1.0 - 0.3e^{-R_t^2}) \tag{2.27}$$

where $C_{2\infty}$ is the high Reynolds number value of C_2 given above, and R_t is a turbulence Reynolds number

$$R_t = \rho k^2/\mu\epsilon \tag{2.28}$$

The constant C_μ is adjusted following Shamroth and Gibeling (Ref. 10)

$$C_\mu = 4a_1^2 \tag{2.29}$$

where a_1 is a function of a different turbulent Reynolds number R_τ, and is given by McDonald and Fish (Ref. 11) as

$$a_1 = a_0\left[\frac{f(R_\tau)}{100}\right] \Bigg/ \left\{1.0 + 6.66\, a_0\left[\frac{f(R_\tau)}{100} - 1\right]\right\} \tag{2.30}$$

In Eq. (2.30) a_0 is taken as 0.0115 and $f(R_\tau)$ is given as (Ref. 11)

$$f(R_\tau) = 100\, R_\tau^{0.22} \qquad R_\tau \le 1 \tag{2.31a}$$

$$f(R_\tau) = 68.1 R_\tau + 614.3 \qquad R_\tau \ge 40 \tag{2.31b}$$

Between the limits $1 < R_\tau < 40$ a cubic is used in the two functional forms given by Eq. (2.31). For these functions R_τ is defined as

$$R_\tau = \frac{\mu_T}{\mu} \tag{2.32}$$

Although the k-ε turbulence model given above provides a general turbulence model in which both the velocity and length scales of turbulence are predicted, the formulation has proven to be unreliable and unduly sensitive to the initial profiles at times leading to the prediction of negative values of k and/or ε. To provide a means of obtaining meaningful

results when such a failure occurs an alternative turbulence model may be used. In this turbulence model a free stream length scale is specified and the turbulence dissipation equation (Eq. 2.24) is not solved. Instead, the turbulence dissipation appearing in (Eq. 2.23) is eliminated using (Eq. 2.26) in conjunction with the specified length scale. In near wall regions the length scale is damped following McDonald and Fish (Ref. 11)

$$\ell = \mathcal{D}\ell_\infty \tanh(\kappa d/\ell_\infty) \tag{2.33}$$

where ℓ_∞ is the freestream length scale, κ is the von Karman constant (=0.43), and $\mathcal{D}$ is a sublayer damping function given as

$$\mathcal{D} = P^{1/2}\left[(d^+ - 23)/8\right] \tag{2.34}$$

Here, P is the normal probability function and $d^+ = du_\tau/\nu$ where u_τ is the friction velocity.

For situations where it might be desirable to investigate the role of turbulence models, a third and very simple turbulence model has been included in the analysis. This turbulence model is referred to as a wake turbulence model and is derived from the definition of turbulent viscosity μ_t, and Prandtl's suggestion that the diffusional flux of some property $\phi = \bar{\phi} + \phi'$ may be expressed

$$-\overline{v'\phi'} = \frac{1}{\sigma_\phi} k^{1/2} \ell \frac{\partial \bar{\phi}}{\partial y} = \frac{\mu_T}{\rho} \frac{\partial \bar{\phi}}{\partial y} \tag{2.35}$$

hence one obtains the Prandtl-Kolmogorov relationship

$$\mu_T = \frac{1}{\sigma_\phi} k^{1/2} \ell \rho \tag{2.36}$$

The wake turbulence model is obtained by assuming that the turbulent length scale and velocity scales are constant throughout the flow field. From equations 2.25 and 2.26 it follows that the constant $1/\sigma_\phi$ is simply $C_\mu^{3/4}$ The velocity scale is taken as the square root of the initially specified turbulence kinetic energy k. The length scale is specified using the geometric constraints of the mixer as a guide, for instance assuming that the initial length scale would not be smaller than the inlet boundary layer or larger than the duct height. As a consequence of this formulation, the turbulent viscosity is dependent only upon the initial choices of k and ℓ, and the local density which is determined as the solution progresses.

APPLICATION TO FLOW IN A LOBE MIXER

In this section, specific details arising in the application of the foregoing analysis to lobe mixer problems are given. A cross section of a typical lobe mixer geometry is shown in Fig. 2. The area immediately downstream of the nozzle plug is faired in with an assumed streamline to model the reversed flow region expected in this region. Since the flow area thus excluded from consideration is very small, this treatment is not believed to introduce significant error. A more detailed analysis of this separated flow region could be performed following a zone embedding approach using the Navier-Stokes equations (cf. [12]). Although the mixer geometry is axisymmetric, the flow is three-dimensional due to the aximuthal variation of the hot and cold streams. However, due to observed symmetry, only a pie-shaped region of the transverse coordinate surface need be considered. The shape of this region and the extent of typical hot and cold streams at the mixer exit surface are shown in Fig. 3.

Coordinate System

Curvilinear orthogonal coordinates x, y, z are constructed to fit the flow passage boundaries downstream of the lobes as shown in Fig. 2. Metric coefficients h_1, h_2, h_3 are defined such that incremental distance s is determined by $(\delta x)^2 = (h_1\delta x)^2 + (h_2\delta y)^2 + (h_3\delta z)^2$. In planes of constant z, (azimuth), orthogonal streamline and velocity potential lines from a two-dimensional planar incompressible potential flow analysis are utilized as the coordinate lines for constant y and x, respectively. This x-y coordinate system is then rotated about an axis representing the centerline of the lobe mixer, to form an axisymmetric coordinate system. Thus, the z direction can be regarded as cylindrical (i.e., θ) and $h_3 = r$. The x coordinate is taken as the primary flow or axial coordinate, and is associated with surfaces for which the two-dimensional potential is constant. The y and z coordinates define transverse secondary flow planes at any given x location. In this coordinate system, the normals $\bar{i}_n$ to the transverse planes coincide with $\bar{i}_1$ the unit vector in the x direction. A two-dimensional incompressible potential flow analysis and computer program developed by Anderson [12] was employed in the present investigation, without modification, to compute the necessary coordinate data.

The Imposed Pressure Field

As discussed in Ref. 1, the axisymmetric coordinate directions generated by rotating planar two-dimensional potential flow coordinates about an axis provides a good approximation for the primary and secondary flow directions, however, the planar two-dimensional potential flow pressure gradients are not suitable for use in approximating the required imposed pressure gradients. Consequently, an incompressible axisymmetric potential flow is computed in the given coordinated system and then scaled for compressibility effects as part of the forward marching solution. In Ref. 1 the compressibility correction was performed using Laitone's rule (Ref. 14), and as a result, inaccuracy at high subsonic Mach number was expected in the correction. This inaccuracy in the imposed pressure field was accepted in Ref. 1 since the main interest in mixing was the immediate region downstream of the lobes and upstream of the throat, and consequently the transonic problem was not a major issue. Under the present effort a more appropriate compressibility scaling based on the work of Lieblein and Stockman (Ref. 15) was developed. Given the incompressible velocity field U_I, Lieblein and Stockman (Ref. 15) demonstrated that an accurate estimate of the compressible flow velocity field could be obtained from the relationship

$$U_c = U_I \left(\frac{\rho_I}{\rho_c}\right)^{(U_I/\bar{U}_I)} \tag{3.1}$$

where U_c is the compressible velocity, ρ_I is the incompressible (or stagnation) density, ρ_c is the local compressible density, and $\bar{U}_I$ is the area averaged incompressible velocity at a given axial location determined as

$$\bar{U}_I = \frac{\int U_I \, dA}{\int dA} \tag{3.2}$$

Lieblein and Stockman suggest that the density ratio, ρ_I/ρ_c be computed using one-dimensional isentropic flow relationships with the Mach number determined by the area ratio. In the present application the density ratio is computed by using the isentropic relationships in conjunction with the local Mach number computed as part of the forward marching solution. In this manner, a fully three-dimensional compressible velocity field can be approximated from the two-dimensional incompressible potential flow. Knowledge of the compressible velocity, and assuming constant total temperature and pressure in the potential flow the static temperature is obtained from

$$T_0 = T - 1/2U_c^2 \tag{3.3}$$

The corrected pressure is then found from the relationship

$$P = P_0(T/T_c)^{\frac{\gamma}{\gamma-1}} \tag{3.4}$$

from which the compressible imposed pressure gradients are determined.

Governing Equations in Orthogonal Coordinates

As in Ref. 1, the governing equations reviewed in the previous section, and the turbulence model equations must be expressed in the orthogonal coordinate system used to represent the mixer passage geometry. Although these equations are fundamentally the same as those presented in Ref. 1, the approximations to the stress terms in the primary momentum equation, and the production term in the turbulence kinetic energy and dissipation rate equations have been altered in an effort to improve the reliability of the k-ε turbulence model. With the exception of these approximations, the equation in orthogonal coordinates follows directly from Eqs. (2.8, 2.9, 2.13, 2.18, 2.20, 2.22, 2.23 and 2.24) by performing the vector operations in the given coordinate system.

Throughout the remaining discussion, all variables in the governing equations are nondimensional, having been normalized by the following reference quantities: distance, L_r; velocity, U_r; density, ρ_r; temperature, T_r; total enthalpy, U_r^2; pressure, $\rho_r U_r^2$; viscosity, μ_r. Here the subscript r denotes a reference quantity. This normalization leads to the following nondimensional parameters: Mach number, M; Reynolds number, Re; Prandtl number, Pr; and specific heat ratio, γ. These parameters are defined by

$$M = U_r/c \ , \ Re = \rho_r U_r L_r/\mu_r \ , \ Pr = c_p \mu_r / k \ , \ \gamma = c_p / c_v \tag{3.5}$$

where μ_r is the molecular viscosity, k is thermal conductivity, and c_p and c_v are the specific heats at constant pressure and volume. The reference speed of sound, c, is defined by $c^2 = \gamma R_g T_r$, where R_g is the gas constant. Since the flow is assumed to be turbulent, the dependent variables are taken to be the time-averaged quantities in the usual sense; however, third order correlation as well as second order correlations including the fluctuating density have been neglected. The decomposition of the velocity vector thus can be written

$$\bar{U} = \bar{i}_1 u + \bar{i}_2 v + \bar{i}_3 w \tag{3.6}$$

Where $\bar{i}_1$, $\bar{i}_2$, and $\bar{i}_3$ are the unit vectors in the x, y, and z coordinate directions, respectively. Since $\bar{i}_1$ is closely aligned with the primary flow direction, v_I is small and is neglected as a minor convenience. This approximation is of little consequence since the neglected quantity v_I effectively reappears as part of v_s and is thus determined from solution of the continuity equation during the forward-marching solution process, instead of being imposed a priori from the potential flow. Since w_I is zero by definition, the velocity decomposition can be written as

$$\bar{u} = \bar{i}_1 u_p + \bar{i}_2 v_s + \bar{i}_3 w_s \tag{3.7}$$

Since u_p is the only streamwise component of $\bar{U}$ the subscript "p" is dropped. Under the stated assumptions the streamwise momentum equation can be written as

$$\begin{aligned}
&\rho u h_2 h_3 \frac{\partial u}{\partial x} + \rho(v_s) h_1 h_3 \frac{\partial u}{\partial y} + \rho(w_s) h_1 h_2 \frac{\partial u}{\partial z} + \rho(v_s) u h_3 \frac{\partial h_1}{\partial y} - \rho(v_s)^2 h_3 \frac{\partial h_2}{\partial x} \\
&- \rho(w_s)^2 h_2 \frac{\partial h_3}{\partial x} + h_2 h_3 \frac{\partial p_I}{\partial x} + h_2 h_3 \frac{dp_v(x)}{dx} = \frac{1}{Re} \frac{\partial}{\partial y}\left[(\mu + \mu_t) \frac{h_1^2 h_3}{h_2} \frac{\partial (u/h_1)}{\partial y}\right] \\
&\frac{h_1 h_2}{Re h_3} \frac{\partial}{\partial z}\left[(\mu + \mu_t) \frac{\partial u}{\partial z}\right] - \frac{2\mu}{Re h_3} \frac{\partial h_3}{\partial z}\left[h_2 \frac{\partial w}{\partial z} + v \frac{\partial h_3}{\partial y}\right] - \frac{2\mu h_3}{Re h_2} \frac{\partial h_2}{\partial x} \frac{\partial v}{\partial y} \\
&- \frac{2\mu}{Re h_1}\left[\frac{h_2}{h_3}\left(\frac{\partial h_3}{\partial x}\right)^2 + \left(\frac{\partial h_2}{\partial x}\right) \frac{h_3}{h_2}\right] u
\end{aligned} \tag{3.8}$$

The energy equation is approximated by

$$\rho u h_2 h_3 \frac{\partial E}{\partial x} + \rho(v_s) h_1 h_3 \frac{\partial E}{\partial y} + \rho(w_s) h_1 h_2 \frac{\partial E}{\partial z}$$
$$= \frac{1}{Re} \frac{\partial}{\partial y}\left[\left(\frac{\mu}{Pr} + \frac{\mu_T}{Pr_T}\right)\frac{h_1 h_3}{h_2}\frac{\partial E}{\partial y}\right.$$
$$\left. + \frac{h_1 h_3}{2h_2}\left(\mu + \mu_T - \frac{\mu}{Pr} - \frac{\mu_T}{Pr_T}\right)\frac{\partial}{\partial y}(\bar{u}^2 + \bar{w}_s^2)\right]$$
$$+ \frac{1}{Re}\frac{h_1 h_2}{h_3}\frac{\partial}{\partial z}\left[\left(\frac{\mu}{Pr} + \frac{\mu_T}{Pr_T}\right)\frac{\partial \bar{E}}{\partial z}\right.$$
$$\left. + 1/2\left(\mu + \mu_T - \frac{\mu}{Pr} - \frac{\mu_T}{Pr_T}\right)\frac{\partial}{\partial z}(\bar{u}^2 + \bar{v}^2)\right] \tag{3.9}$$

with the Prandtl number Pr and turbulent Prandtl number Pr_T assumed to be 1.0.

To obtain the rotational secondary flow components of the velocity, the streamwise vorticity equation is written as

$$\frac{u}{Q}\left(\rho u \frac{\partial \xi}{\partial x} - \xi \frac{\partial \rho u}{\partial x}\right) + \frac{v_s}{Q}\frac{h_1}{h_2}\left(\rho u \frac{\partial \xi}{\partial y} - \xi \frac{\partial \rho u}{\partial y}\right) + \frac{w_s}{Q}\frac{h_1}{h_3}\left(\rho u \frac{\partial \xi}{\partial z} - \xi \frac{\partial \rho u}{\partial z}\right)$$
$$= -\frac{2}{h_2}\frac{\partial h_1}{\partial y}\rho u \frac{1}{h_3}\frac{\partial u}{\partial z} - \frac{h_1}{h_2 h_3}\frac{1}{\rho}\left[\frac{\partial P}{\partial y}\frac{\partial \rho}{\partial z} - \frac{\partial \rho}{\partial y}\frac{\partial P}{\partial z}\right]$$
$$+ \frac{\rho}{Re}\left\{\frac{h_1}{h_2 h_3}\frac{\partial}{\partial y}\left[\frac{h_3}{h_1 h_2 \rho}\frac{\partial h_1(\mu+\mu_T)\xi}{\partial y}\right] + \frac{h_1}{h_3^2}\frac{\partial}{\partial z}\left[\frac{1}{\rho}\frac{\partial(\mu+\mu_T)\xi}{\partial z}\right]\right\} \tag{3.10}$$

where $Q^2 = u^2 + v_s^2 + w_s^2$ and the vorticity is related to velocity by

$$\xi = \frac{1}{h_2 h_3}\left(\frac{\partial h_3 w_s}{\partial y} - \frac{\partial h_2 v_s}{\partial z}\right) \tag{3.11}$$

The vector potential $\bar{\psi}_s$ is determined from

$$\frac{1}{h_2 h_3}\frac{\partial}{\partial y}\left[\left(\frac{h_3}{\rho h_1 h_2}\right)\frac{\partial(h_1\psi_s)}{\partial y}\right] + \frac{1}{h_1 h_3^2}\frac{\partial}{\partial z}\left[\left(\frac{1}{\rho}\right)\frac{\partial(h_1\psi_s)}{\partial z}\right] = -\xi \qquad (3.12)$$

and the rotational secondary flow velocities are determined as

$$v_\psi = \frac{1}{\rho h_1 h_3}\frac{\partial(h_1\psi_s)}{\partial z} \qquad (3.13a)$$

$$w_\psi = -\frac{1}{\rho h_1 h_2}\frac{\partial(h_1\psi_s)}{\partial y} \qquad (3.13b)$$

The scalar potential is governed by

$$\frac{\partial}{\partial y}\left[\frac{\rho h_1 h_3}{h_2}\frac{\partial\phi_s}{\partial y}\right] + \frac{\partial}{\partial z}\left[\frac{\rho h_1 h_2}{h_3}\frac{\partial\phi_s}{\partial z}\right] = -\frac{\partial(h_2 h_3 \rho u)}{\partial x} \qquad (3.14)$$

The velocity components v_ϕ and w_ϕ are found to be

$$v_\phi = \frac{1}{h_2}\frac{\partial\phi_s}{\partial y} \qquad (3.15a)$$

$$w_\phi = \frac{1}{h_3}\frac{\partial\phi_s}{\partial z} \qquad (3.15b)$$

The secondary flow velocities are thus

$$v_s = v_\psi + v_\phi \qquad (3.16a)$$

$$w_s = w_\psi + w_\phi \qquad (3.16b)$$

The turbulence model equations must also be expressed in orthogonal coordinates. It is assumed that the turbulence equations are tensor invariant [9], and thus may be expressed directly in orthogonal coordinates by performing vector operations in such a coordinate system. With streamwise diffusion neglected to allow forward-marching solution, the result for the turbulence kinetic energy equation in steady flow is

$$\rho u h_2 h_3 \frac{\partial k}{\partial x} + \rho v_s h_1 h_3 \frac{\partial k}{\partial y} + \rho w_s h_1 h_2 \frac{\partial k}{\partial z} = \frac{1}{Re}\left\{ \frac{\partial}{\partial y}\left[\frac{h_1 h_3}{h_2}\left(\mu + \frac{\mu_T}{\sigma_k}\right)\frac{\partial k}{\partial y}\right] + \frac{h_1 h_2}{h_3}\frac{\partial}{\partial z}\left[\left(\mu + \frac{\mu_T}{\sigma_k}\right)\frac{\partial k}{\partial z}\right]\right\} - h_1 h_2 h_3 \rho \epsilon + P \tag{3.17}$$

and similarly the turbulence dissipation equation is given by

$$\rho u h_2 h_3 \frac{\partial \epsilon}{\partial x} + \rho v_s h_1 h_3 \frac{\partial \epsilon}{\partial y} + \rho w_s h_1 h_2 \frac{\partial \epsilon}{\partial z} = \frac{1}{Re}\left\{ \frac{\partial}{\partial y}\left[\frac{h_1 h_3}{h_2}\left(\mu + \frac{\mu_T}{\sigma_\epsilon}\right)\frac{\partial \epsilon}{\partial y}\right] + \frac{h_1 h_2}{h_3}\frac{\partial}{\partial z}\left[\left(\mu + \frac{\mu_T}{\sigma_\epsilon}\right)\frac{\partial \epsilon}{\partial z}\right]\right\} - h_1 h_2 h_3 C_2 \rho \frac{\epsilon^2}{k} + C_1 \frac{\epsilon}{k} P \tag{3.18}$$

The production term is approximated as

$$P = \frac{\mu_T}{Re}\left\{ 2\left[v\left(\frac{\partial h_1}{\partial y}\right)\frac{1}{h_1 h_2}\right]^2 + 2\left[\frac{1}{h_3}\frac{\partial w}{\partial z} + u\frac{\partial h_3}{\partial x}\left(\frac{1}{h_1 h_3}\right) + v\frac{\partial h_3}{\partial y}\left(\frac{1}{h_2 h_3}\right)\right]^2 + \left[\frac{h_1}{h_2}\frac{\partial (u/h_1)}{\partial y}\right]^2 + \left[\frac{h_3}{h_2}\frac{\partial (w/h_3)}{\partial y} + \frac{1}{h_3}\frac{\partial v}{\partial z}\right]^2 + \left[\frac{1}{h_3}\frac{\partial u}{\partial z}\right]^2 \right. \tag{3.19}$$

The turbulent viscosity is then

$$\mu_T = \frac{C_\mu \rho k^2}{\epsilon} Re \tag{3.20}$$

and the length scale may be determined as

$$\ell = \frac{C_\mu^{3/4} k^{3/2}}{\epsilon} \tag{3.21}$$

When the k-ℓ turbulence model is used, Eqs. (3.19) and (3.20) are combined to eliminate the appearance of the turbulent dissipation from Eq. (3.19).

$$\epsilon = C_\mu^{3/4} k^{3/2} / \ell \tag{3.22}$$

and it follows that

$$\mu_t = C_\mu^{1/4} k^{1/2} \ell \, Re \tag{3.23}$$

Specification of Initial Conditions

The initial conditions for a lobe mixer calculation may be specified by using either an automated starting routine or by reading in experimental data. The fully automated procedure is considered first.

To obtain initial conditions for a lobe mixer calculation, it is necessary to specify the velocity and total temperature of the respective hot and cold streams in addition to a mean value of static pressure. The lobe shape is specified, and based on the specified lobe shape, a decision is made as to whether a grid point lies in the hot or cold stream. The appropriate values for velocity, temperature and density are then assigned to the grid point. The total energy is assumed to be constant but may differ in both streams. The velocity in the two respective streams is assigned its nondimensional reference value which is then corrected to account for normal pressure gradients present at the initial plane as determined from the axisymmetric potential flow. To account for boundary layers on the lobe, hub and shroud surfaces, the free stream velocity profiles are further scaled in accordance with an assumed turbulent boundary layer velocity profile, and the distance from the surface. Radial secondary flow velocities at the initial station may be specified parametrically in each stream as a fraction of the streamwise velocity. This in effect sets the flow angle in the fan and turbine streams, respectively. Finally, a swirl velocity component may be specified, when appropriate.

The initial velocity profile with boundary layers is given by

$$u = u(u_{STRM}, \delta_{BL}, y/\delta_{BL}, \delta^*, H) \tag{3.24}$$

where U_{STRM} is the velocity of the appropriate stream, δ_{BL} is the boundary layer thickness, y/δ_{BL} represents the shortest distance from a surface (hub, shroud or lobe) to the grid point in question, δ^* is the local displacement thickness and H is the shape factor. The assumed boundary layer profile used in the present code is a Coles-type profile modified as suggested by Walz [16].

$$u = u_\tau\left[(-3y^+ - 5)e^{-3y^+} + \frac{1}{\kappa}\ln(1+y^+) + C + \frac{\Pi}{\kappa} w\left(\frac{y}{\delta}\right)\right] \tag{3.25}$$

In Eq. (3.25) C is a constant taken as 5.0, Π is a parameter which determine the strength of the wake component of the velocity profile, and w is Coles wake function [16].

Following [4], the radial component of velocity in the fan or turbine stream is then given as

$$v = u\,\alpha_{fan} \tag{3.26}$$

for the fan stream and

$$v = u\,\alpha_{core} \tag{3.27}$$

for the turbine stream where α is defined as a mean flow angle.

Finally, the swirl velocity is specified in terms of a mean swirl velocity magnitude and by specifying the radial limits over which there is to be swirl as an initial condition. The swirl velocity at the initial station (but only at the initial station) is assumed constant in the azimuthal direction. This condition could be changed at an arbitrary inlet swirl profile, if required, but is adopted here for convenience.

The majority of calculations to be performed with the present code are expected to be run without resolving the hub and casing boundary layers. For these cases, the initial velocity field in the immediate vicinity of solid surfaces must be treated in an approximate manner. This is accomplished by using wall functions which assume that locally between the wall and the first grid point away from the wall the velocity profile is logarithmic such that

$$u = u_\tau\left(\frac{1}{\kappa}\ln\frac{u_\tau y}{\nu} + C\right) \tag{3.28}$$

where u_τ is the friction velocity, $\kappa = 0.43$ is the von Karman constant, and c is taken as 5.0. It follows that

$$\frac{\partial u}{\partial y} = \frac{u_\tau}{\kappa y} \tag{3.29}$$

Equation (3.28) is used to determine a wall slip velocity such that the finite differenced form of the velocity gradient one point off the wall is consistent with the assumed law of the wall profiles. When wall functions are used to represent the primary flow velocity, the secondary flow velocities are still required to obey no slip conditions. Thus in the near wall regions the secondary flow velocity is assumed to vary from zero to its free stream value in a cubic manner with distance from the nearest wall across some specified secondary flow boundary layer thickness. Once the velocity and temperature distribution are set up, the density is computed to be consistent with the temperature and local static pressure as determined from the mean static pressure corrected for the normal pressure gradients.

Initial conditions for the turbulence model are determined through specification of a reference length scale, ℓ_{ref} and free stream turbulence levels. Near the hub and shroud the length scale is determined from the McDonald-Camarata [17] relationship

$$\ell = \ell_{ref} \tanh\left(\frac{\kappa y}{\ell_{ref}}\right) \tag{3.30}$$

where y is the distance from the surface in question. In the region about the lobe surface, the distribution of Eq. (3.30) may be used with y representing the distance to the lobe from the grid point in question. However, since the lobe may pass arbitrarily close to a grid point the length scale determined from Eq. (3.30) will approach 0.0 as y approaches 0.0. This results in a low Reynolds number region in the initial flow field which can create problems with the turbulence model. This problem is circumvented through use of an option which renders the length scale constant in the region near the lobe, and the distribution of Eq. (3.30) is used only near the hub or casing if boundary layers are specified there. With the length scale distribution known, the initial turbulent viscosity is obtained from the generalized mixing length relationship

$$\mu_T = \rho \ell^2 \left[\left(\frac{1}{h_2}\frac{\partial \bar{u}}{\partial y}\right)^2 + \left(\frac{1}{h_2}\frac{\partial \bar{w}}{\partial y}\right)^2 + \left(\frac{1}{h_3}\frac{\partial \bar{u}}{\partial z}\right)^2 + \left(\frac{1}{h_3}\frac{\partial \bar{v}}{\partial z}\right)^2\right]^{1/2} \tag{3.31}$$

The initial turbulence kinetic energy and dissipation are then determined from simultaneous solution of Eqs. (2.25) and (2.26). The kinetic energy is modified slightly following McDonald and Kreskovsky [18] to account for the free stream turbulence, and the turbulent viscosity is then recomputed from k and ε to be consistent.

Under certain conditions, neither the wall length scale option Eq. (3.30) nor the wake length scale option (constant length scale) will provide satisfactory initial values of k, ε and μ_T. This may occur when the mesh is coarse and the velocity gradients in Eq. (3.31) vary greatly between adjacent grid points. Under these circumstances, it is useful to initiate the turbulence quantities using an option which specifies the turbulent kinetic energy, dissipation and viscosity as essentially constant throughout the flow field. Such an approach has also been used previously by Launder, Morse, Rodi and Spalding [11] in the computation of free shear flows.

If experimental profiles are read in, the specification of initial conditions is similar. The velocity components and static temperature are input at each grid point. The lobe shape is specified as in the automated starting procedure, and a reference length scale and free stream turbulence intensities must be provided. Additionally, estimates of the boundary layer thickness on the hub, shroud and lobe must be specified for use in setting up the initial turbulence quantities. Initialization of the turbulence quantities is similar to that used in the automated procedure.

Boundary Conditions

To march the solution downstream, it is necessary to apply boundary conditions in each transverse plane. Boundary conditions are needed for the energy equation, the primary flow momentum equation, the streamwise vorticity equation, the vector and scalar potential equations, and the turbulence model equations. The boundary conditions will in general depend on whether swirling or nonswirling flow is considered, and whether or not wall boundary layers are considered. Referring to Fig. 4, the boundaries at θ_{min} and θ_{max} represent either symmetry planes or periodic surfaces. Boundaries at the hub (or centerline) and shroud surfaces require conditions appropriate for solid surfaces (hub or shroud) or a centerline (symmetry).

Nonswirling Flows

For nonswirling flows boundary conditions along θ_{min} and θ_{max} are specified as follows:

1) aximuthal gradients of U_p, E, k and ϵ are set to zero
2) the vorticity is set to zero, and
3) the normal velocity component is zero, thus the vector potential is zero and the azimuthal gradient of the scalar potential is zero.

Boundary conditions on the hub and shroud surface are specified as follows:

1) the normal velocity is zero along these surfaces, and the vector potential and the normal gradient of the scalar potential are thus set to zero, and
2) these surfaces are taken as adiabatic, and thus the normal gradient of enthalpy is set to zero.

For the majority of calculations it is not expected that the wall boundary layer will be resolved. Thus, the appropriate boundary condition for the

primary flow velocity, U_p, is the gradient condition of Eq. (3.29). For the turbulence quantities k and ε boundary conditions consistent with the log law are

$$k = \frac{U_\tau^2}{c_\mu^{1/2}} \tag{3.32}$$

which is used to replace Eq. (3.31) one point off a wall and then

$$\frac{\partial k}{\partial y} = 0 \tag{3.33}$$

is specified on the wall. For ε the condition

$$\varepsilon = \frac{U_\tau^3}{\kappa y} \tag{3.34}$$

is used. The use of Eqs. (3.32 and 3.34) effectively sets the turbulent viscosity one point off a wall consistent with the log law. If boundary layers are resolved, then $U_p = k = \varepsilon = 0$ on solid walls is specified.

With regard to the boundary conditions for the secondary vorticity, in Ref. 1 it was argued that a zero vorticity boundary condition would be suitable for use with the wall function approach to the primary flow. Although this was satisfactory in many cases, in some instances it gave rise to large tangential velocity components on the hub or shroud surfaces. As a result, under the present modifications of the code the secondary flow vector potential and vorticity equations are solved using a coupled solution procedure. This procedure allows specification of the correct coupled stream function-vorticity boundary condition which ensures that the secondary flow velocity components obey no slip on solid walls.

Swirling Flows

With the exception of the vector potential, boundary conditions on the hub and shroud surfaces remain unchanged for swirling flow. Special treatment must be given to vector potential, however, because flow may pass in and out of the computational region along the radial lines at θ_{min} and θ_{max}. The amount of flow crossing these radial lines is due to the swirl velocity, and a means of determining the growth or decay of the swirl must be accounted for. This is accomplished by solving a θ-momentum equation along one of the radial coordinate lines prior to solving the secondary flow vorticity-vector potential system. The resulting prediction of the θ velocity component can be integrated to obtain the difference in the stream function between hub and shroud boundaries due to swirl,

$$\Delta\psi = \int \rho(w - w_\phi)\, h_1\, h_2\, dy \qquad (3.35)$$

which provides the necessary information for the boundary conditions. In Eq. (3.35), w_ϕ is subtracted from w, consistent with Eq. (2.3), since the velocity predicted from solution of the θ momentum equation contains both rotational and irrotational components. With regard to the boundary conditions in the azimuthal θ direction, all flow variables are assumed to be periodic.

COMPUTED RESULTS

Several test calculations were performed to demonstrate the extended capability of the modified computer code. The test cases were all performed for the geometry shown in Fig. 2 immediately downstream of the lobes with the lobe shape shown in Fig. 3. A summary of initial condition for each case is given in Table I. As can be seen in Table I these test cases were run with a variety of conditions to demonstrate the effect of secondary flows of various magnitudes, the effect of swirl, and the effects of the various turbulence models.

Before discussing results from these calculations, it is useful to define average values of total pressure loss coefficient, ideal thrust coefficient, and Mach number at each axial location, to aid in the evaluation of flow properties. A mass-averaged total pressure loss coefficient C_{PT} is defined as

$$C_{PT} = \frac{\int_A \frac{2(P_{T_{ref}} - P_T)}{(\rho u^2)_{ref}} \rho \bar{U} \cdot d\bar{A}}{\int_A \rho \bar{U} \cdot d\bar{A}} \tag{4.1}$$

where $P_{T_{ref}}$ is a reference total pressure associated with the turbine stream reference conditions, and ρ_{ref} and u_{ref} are the reference density and velocity associated with the turbine stream. The value of C_{PT} at the starting plane is usually not zero due to the presence of shear layers in the initial conditions, and for clarity this starting value is subtracted from C_{PT} in the presentation of results. The distributions of C_{PT} presented thus represent losses incurred downstream of the starting plane. An ideal thrust coefficient is defined and based on the thrust which would be obtained by isentropic expansion from local conditions to a predetermined exit pressure. The ratio of the local value of this thrust T to the value T_i based on the initial flow field is defined as the ideal thrust coefficient, T/T_i. The thrust is obtained from the relationship

$$T = \int_{A_e} \gamma P_e M_e^2 dA_e \tag{4.2}$$

where P_e is the assumed exit pressure, $\bar{M}_e$ is the Mach number based on isentropic expansion from the local pressure to P_e, and $\bar{A}_e$ is the effective exit area, again based on isentropic expansion to P_e.

Effects of Secondary Flows

The effects of the magnitude of the initial secondary flows prescribed at the lobe exit was investigated by performing two calculations designated as case I and case II in Table I, where the initial conditions are summarized. In the case I calculation, a radial inward velocity equal to 13% of the local fan stream velocity was specified. In the turbine stream, a radial outward velocity of 8% was specified. The case II calculation had fan and turbine streams radial velocities specified as 20% and 25%, respectively. Both calculations used the new optional k-ℓ turbulence model, thus the calculations also serve to demonstrate this capability.

The relative effects of the different initial secondary flow on mixing are best examined by looking at the total temperature contours at the nozzle exit plane. As noted in Table I, the temperature ratio between the streams is different for cases I and II, however, in the absence of initial secondary flows the thermal mixing between the two streams results in a 'tear drop' total temperature pattern (c.f. Ref. 3). The departure from this 'tear drop' pattern thus indicates the degree to which initial secondary flows effect the mixing process, even though these two cases have different initial temperature ratios. The total temperature contours are shown in Fig. 5. The case I results show a small but significant departure from the 'tear drop' total temperature pattern observed when no secondary flow is specified at the initial plane. However, the results for case II, where even larger secondary flows are specified at the initial plane, show a much more dramatic distortion of the total temperature contours at the nozzle exit. Here the hot fluid in the upper portion of the lobe is effectively pinched off from that in the lower portion of the same lobe, and a classical mushroom-shaped pattern (c.f. Refs. 4 and 5), indicating the presence of strong counter-rotating vortices is observed. These results clearly demonstrate the important effects of vorticity or secondary flows in the initial conditions, and indicate the importance of lobe generated secondary flow on the temperature profile development.

Effects of Turbulence Models

The influence of the various turbulence models, k-ε, k-ℓ or the wake model were investigated by rerunning case II with the k-ε and wake turbulence models as cases III and IV, respectively. With the exception of the turbulence model used, cases II, III and IV are identical as can be observed in Table I. The results of these calculations are summarized in Table II where area-averaged values of total pressure ratio, and total temperature ratio are presented along with the previously defined total pressure loss coefficient, and thrust ratio. Examination of the infor-

mation presented in Table II indicates that the computed results for this lobe mixer flow show only very limited variation with the turbulence model. The results indicated that the k-ε model gives the higher losses whereas the wake model predicts the lowest. In view of this limited dependence on turbulence model, it would appear that turbulence modeling in lobe mixers is not an area of primary importance. This is born out further by the comparisons presented in Fig. 6 where the total temperature signatures resulting from each calculation are shown. This comparison shows that only small scale details are altered by the different turbulence models while the large scale features remain unaffected. Additional evidence that turbulence modeling may not be of primary importance in lobe mixer flows is provided in Fig. 7 where the secondary flow vorticity contours at the nozzle exit are compared for the three turbulence models. Here also, it is observed that the predicted vorticity contours for all three turbulence models are nearly identical. The pattern of two large counter-rotating vorticities is observed for all three turbulence models, and the strength and size of these vorticities remain uneffected by the turbulence model used. Some small differences in the contours are observed, however, particularly when using the k-ℓ turbulence model. These small scale differences appear as slight distortions of the vortex contours, but as indicated in Table II, this effect does not apparently alter the mixing in any significant manner.

Effect of Swirl

Perhaps the most significant modification to the computer code performed under the present effort is the extension of the capability of the code to swirling flow. To demonstrate this capability several computations were carried out for swirling flows. The first of these calculations, case V, is identical to case III discussed previously with the additional specification of an initial swirl component of velocity, equal to 10% of the hot stream velocity, across the entire mixing duct (hub to shroud). The pertinent integrated quantities for these two calculations are presented in Table III.

As would be expected, case V with swirl exhibits higher losses reflected by the area averaged total pressure ratio and the total pressure loss coefficient, and a lower thrust ratio. The contour plots of the exit plane total temperature distribution for these two cases is shown in Fig. 8. This comparison demonstrates that the large scale features of the signature remain almost unaltered by swirl and are simply convected in the azimuthal direction. Some distortion of the pattern is observed, particularly as the center of the mixing duct is approached;

however, these effects do not appear to enhance the mixing of the two streams significantly. A comparison of the vorticity contours at the nozzle exit plane, shown in Fig. 9, indicates a more substantial distortion of the counter rotating vortex pair by swirl. This suggests that in longer mixing ducts, where swirl effect may develop further, more significant effects on mixing may be observed. However, in view of the higher losses incurred with swirl, and the absence of any clear-cut benefits resulting from swirl, it would appear that swirl in lobe mixers may not be beneficial from a performance standpoint.

A final calculation with swirl, case VI, was made using the wake turbulence model, and with 10% swirl velocity confined to the outer half of the mixing duct. This calculation was made to determine if residual swirl in the fan stream would alter the mixing significantly. The exit plane total temperature contours for this calculation are presented in Fig. 10. Again, no significant effect on mixing is observed. The large scale characteristics of the total temperature signature remain intact with some distortion observed in the outer region of the flow.

Although swirl did not appear to have a significant effect on the mixing characteristics of the lobe mixer/exhaust nozzle used in the present calculation, it should be noted that the exhaust nozzle was short. If a longer exhaust nozzle were used, the effects of swirl would have more time to develop, and significant effects on mixing could result. However, as noted earlier, swirl does appear to give rise to higher losses, and if performance is the objective, swirl does not appear to be beneficial.

SUMMARY AND CONCLUSIONS

An analysis which was previously developed for detailed prediction and computation of three-dimensional subsonic turbulent flows in turbofan lobe mixers has been extended and modified. An improved starting procedure which allows specification of non-zero starting vorticity using a parametric representation of radial flow velocities at the initial plane has been developed. The method of scaling an incompressible potential flow to obtain the compressible flow imposed pressure gradients has been improved. An optional k-ℓ turbulence model has been incorporated within the code, and the original k-ϵ turbulence model has been modified to provide improved reliability. Finally, a swirling flow capability has been added to the code.

Calculations have been performed for a number of test cases to verify the modifications to the code, and to demonstrate the importance of the effects of secondary flows, turbulence model, and swirl on mixing. The results of these calculations indicate that secondary flows generated within the lobes play the most dominant role in determining the degree of mixing. The effects of the turbulence model appears to play a very limited role, altering only small scale details of the predicted flow field. Finally, calculations where a swirl component of velocity, equal to 10% of the turbine stream velocity, was specified across the entire mixing duct indicated that swirl may not alter the degree of mixing substantially. In this case, the major effect was to simply rotate the total temperature pattern observed without swirl with little additional distortion. However, specifying swirl over a limited portion of the duct radial extent may have a more pronounced effect. More detailed investigations and experimental confirmation will be required to fully assess these effects.

REFERENCES

1. Kreskovsky, J.P., Briley, W.R. and McDonald, H.: Turbofan Forced Mixer-Nozzle Internal Flow Field III-A Computer Code for 3-D Mixing in Axisymmetric Nozzles. NASA CR 3494, April 1982.

2. Kreskovsky, J.P., Briley, W.R. and McDonald, H.: Prediction of Laminar and Turbulent Primary and Secondary Flows in Strongly Curved Ducts, NASA CR3388, February 1981.

3. Povinelli, L.A., Anderson, B.H. and Gerstenmaier, W.H.: Computation of Three-Dimensional Flow in Turbofan Mixers and Comparison with Experimental Data, AIAA Paper No. 89-0227, January 1980.

4. Anderson, B.H., Povinelli, L.A. and Gerstenmaier, W.H.: Influence of Pressure Driven Secondary Flows on the Behavior of Turbofan Forced Mixers, AIAA Paper No. 89-1198, June 1980.

5. Anderson, B.H. and Povinelli, L.A.: Factors Which Influence the Behavior of Turbofan Forced Mixer Nozzles. NASA TM 81668, January 1981.

6. Briley, W.R.: Numerical Method for Predicting Three-Dimensional Steady Viscous Flow in Ducts. J. Comp. Phys., Vol. 14, 1974, p. 8.

7. Patankar, S.V. and Spalding, D.B.: A Calculation Procedure for Heat, Mass, and Momentum Transfer in Three-Dimensional Parabolic Flows. Int. J. Heat and Mass Transfer, Vol. 15, 1972, p. 1787.

8. Lakshminarayana, B. and Horlock, J.H.: Generalized Expressions for Secondary Vorticity Using Intrinsic Coordinates. J. Fluid Mech., Vol. 59, 1973, p. 97.

9. Launder, B.E. and Spalding, D.B.: The Numerical Computation of Turbulent Flows. Computer Methods in Applied Mechanics and Engineering, Vol. 3, 1974, p. 269.

10. Shamroth, S.J. and Gibeling, H.J.: The Prediction of the Turbulent Flow Field about an Isolated Airfoil, AIAA Paper 79-1543, 1979.

11. McDonald, H. and Fish, R-W.: Practical Calculations of Transitional Boundary Layers, Int. J. Heat and Mass Transfer, Vol. 16, 1979, p. 1729.

12. McDonald, H. and Briley, W.R.: Computational Aspects of Internal Flows, AIAA Paper No. 79-1445, 1979.

13. Anderson, O.L.: User's Manual for a Finite-Difference Calculation of Turbulent Swirling Comptessible Flow in Asixymmetric Ducts with Struts and Slot Cooled Walls. USAAMRDL-TR-74-50, Vol. I, 1974.

14. Shapiro, A.H.: The Dynamics and Therodynamics of Compressible Fluids Flow, Vol. I. Ronald Press, New York, 1955.

15. Lieblein, S. and Stockman, N.O.: Compressibility Correction for Internal Flow Solutions. J. Aircraft, Vol. 9, No. 4, 1972, p. 312.

16. Walz, A.: Boundary Layers of Flow and Temperature. MIT Press, 1969, p. 115.

17. McDonald, H. and Camarata, F.J.: An Extended Mixing Length Approach for Computing the Turbulent Boundary-Layer Development. In Proceedings, Stanford Conference on Computation of Turbulent Boundary Layers, Vol. I, published by Stanford University, 1969, pp. 83-98.

18. McDonald, H. and Kreskovsky, J.P.: Effect of Free-Stream Turbulence on the Turbulent Boundary Layer. International Journal of Heat and Mass Transfer, Vol. 17, No. 7, 1974, p. 705.

19. Launder, B.E., Morse, A., Rodi, W. and Spalding, D.B.: Prediction of Free Shear Flows - A Comparison of the Performance of Six Turbulence Models. NASA SP-321, Vol. I, 1972, p. 361-426.

TABLE I

CASE #	U_F/U_T	T_F/T_T	V_F	V_T	W_S	ℓ	k	TURB MOD	Re
1	.633	.4	-.13	.08	0	.006	.04	k-ℓ	1.13×10^6
2	.86	.74	-.20	.25	0	.006	.04	k-ℓ	1.13×10^6
3	.86	.74	-.20	.25	0	.006	.04	k-ε	1.13×10^6
4	.86	.74	-.20	.25	0	.006	.04	WAKE	1.13×10^6
5	.86	.74	-.20	.25	.1 full	.006	.04	k-ε	1.13×10^6
6	.86	.74	-.20	.25	.1 outer half	.006	.04	WAKE	1.13×10^6

U_F = Fan stream velocity

U_T = Turbine stream velocity

T_F = Fan stream temperature

T_T = Turbine stream temperature

V_F = Fan stream radial velocity

V_T = Turbine stream radial velocity

W_s = Swirl velocity

ℓ = Turbulence length scale

k = Turbulence kinetic energy

Re = Reynolds number

TABLE II

CASE	TURBULENCE MODEL	TOTAL PRESSURE RATIO	TOTAL TEMP. RATIO	C_{PT} LOSS = (+)	THRUST RATIO
II	k-ℓ	.9892	.7866	.0956	.9930
III	k-ε	.9890	.7863	.0975	.9926
IV	WAKE	.9896	.7866	.0923	.9933

TABLE III

CASE	TURBULENCE MODEL	TOTAL PRESSURE RATIO	TOTAL TEMP. RATIO	C_{PT} LOSS = (+)	THRUST RATIO
III	k-ε	.9890	.7863	.0975	.9926
V	k-ε	.973	.7884	.1132	.9883

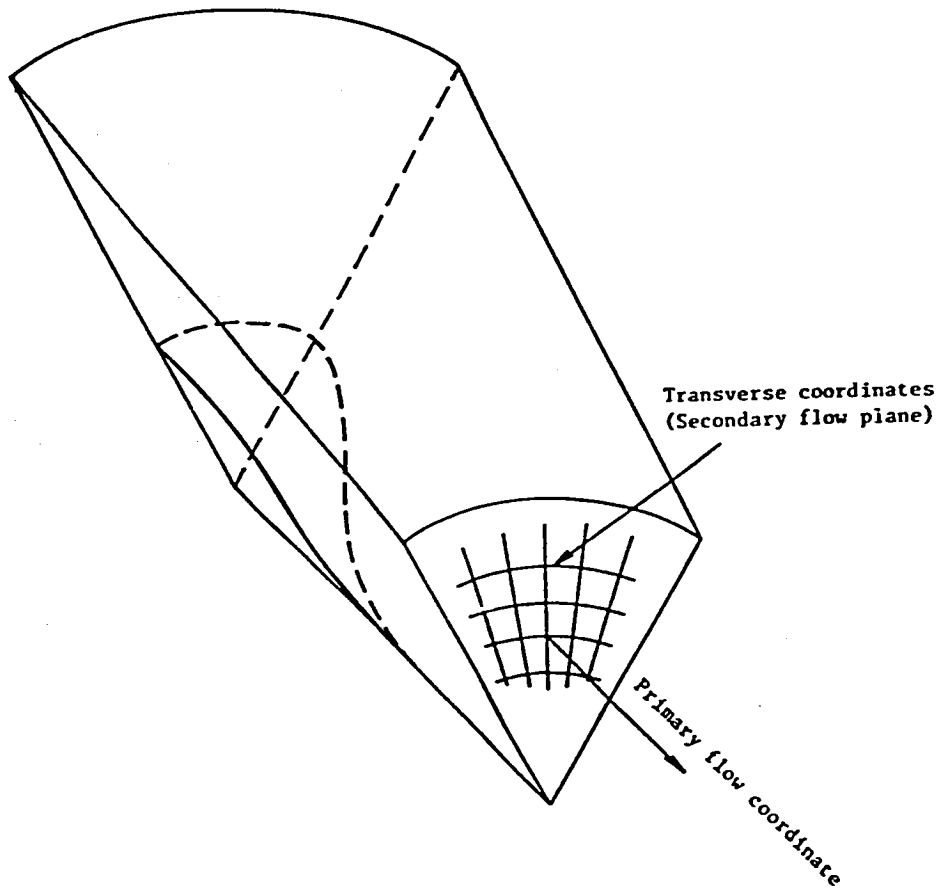

Figure 1. – Schematic of coordinate system for three-dimensional flow problem.

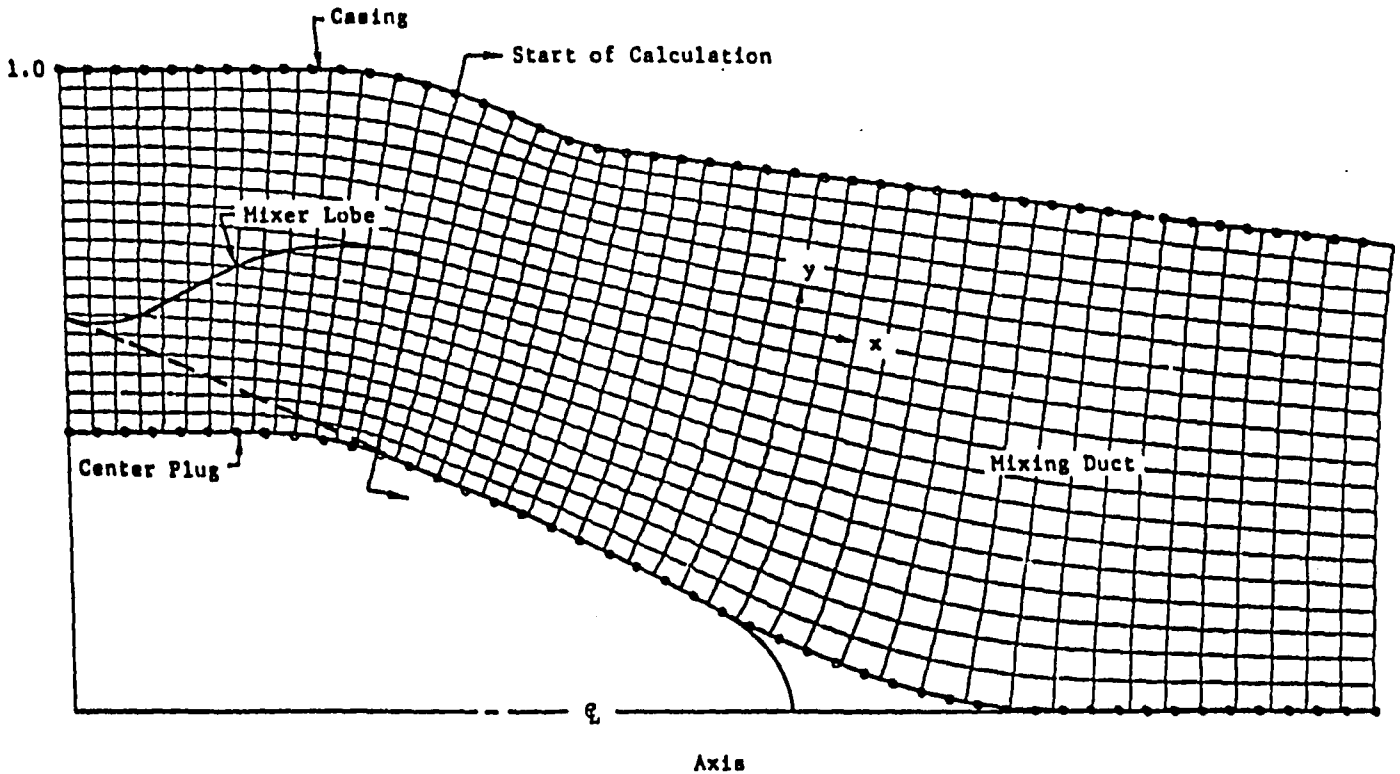

Figure 2. - Typical lobe mixer geometry and potential flow coordinate system.

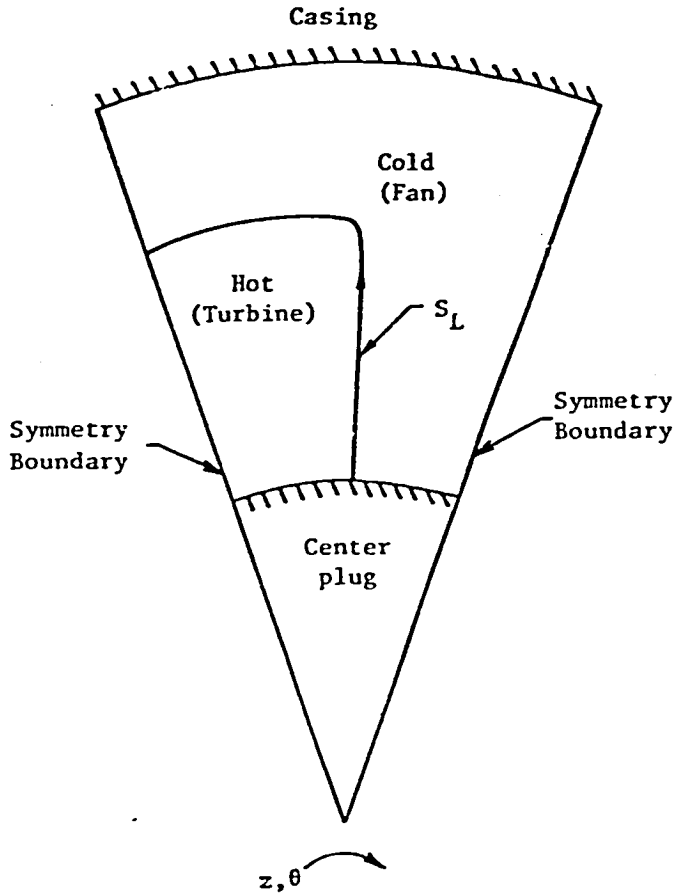

Figure 3. - Typical cross section at mixer exit surface.

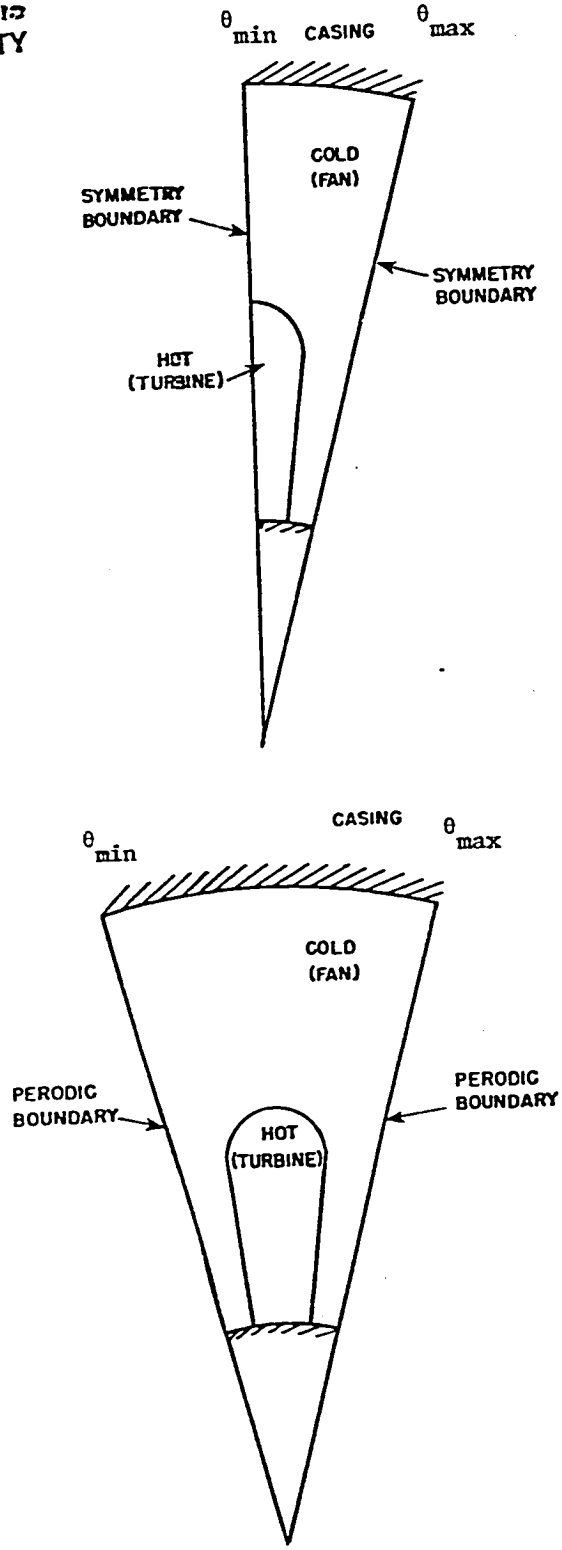

Fig. 4 - Boundary conditions for flows with and without swirl.

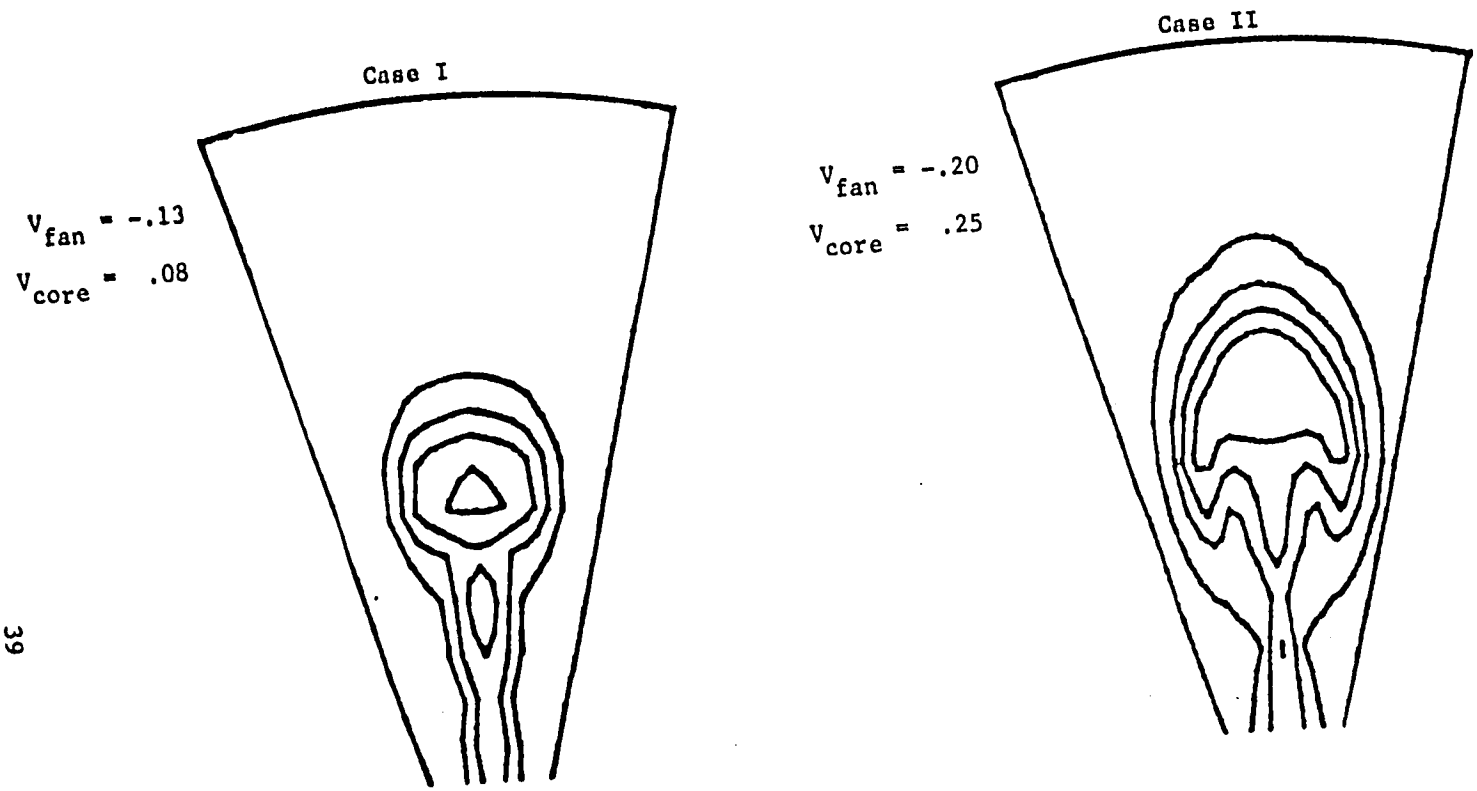

Fig. 5 - Effect of initial secondary flows on exit plane total temperature contours.

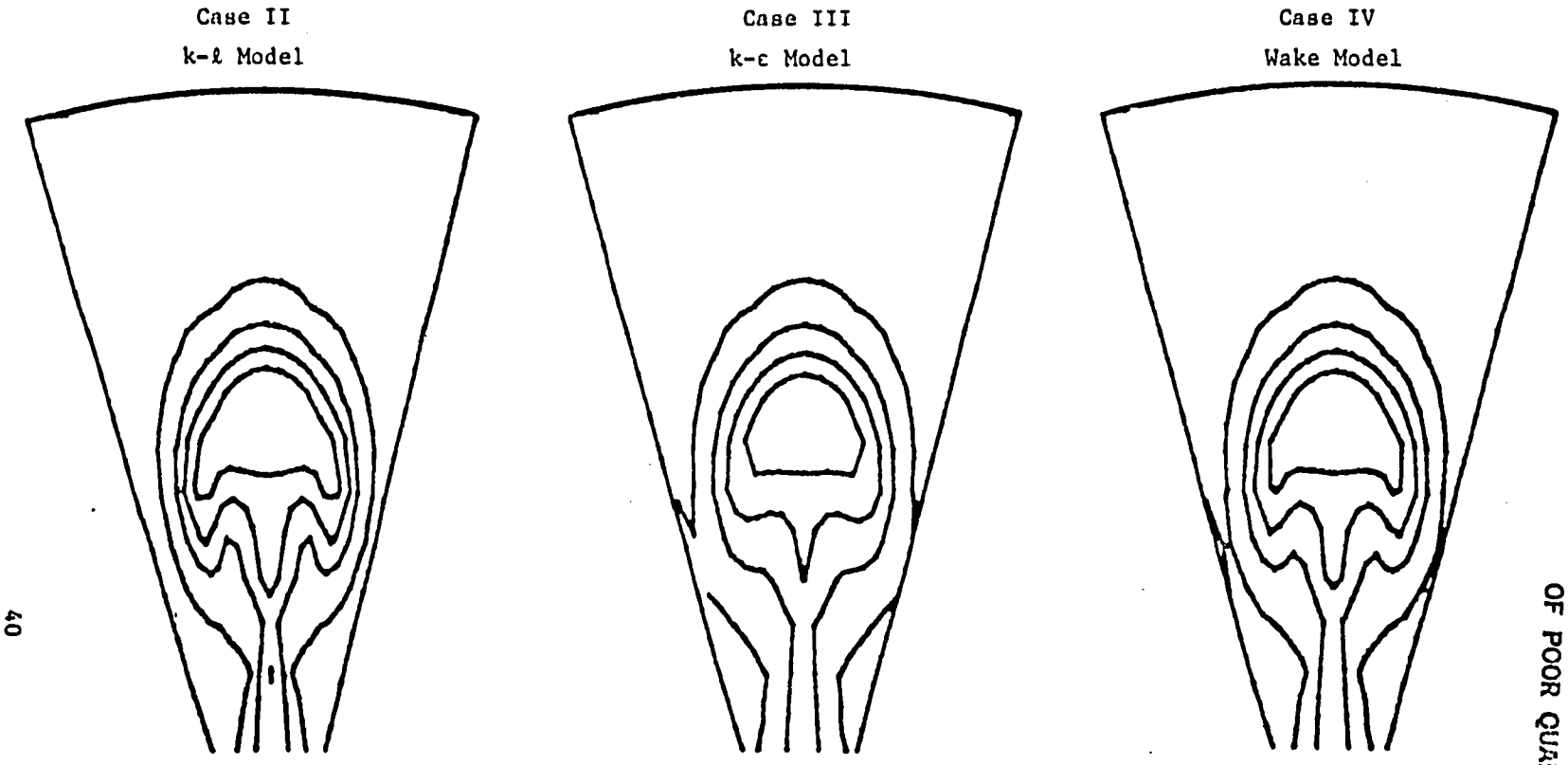

Fig. 6 - Effect of turbulence model on exit plane total temperature contours.

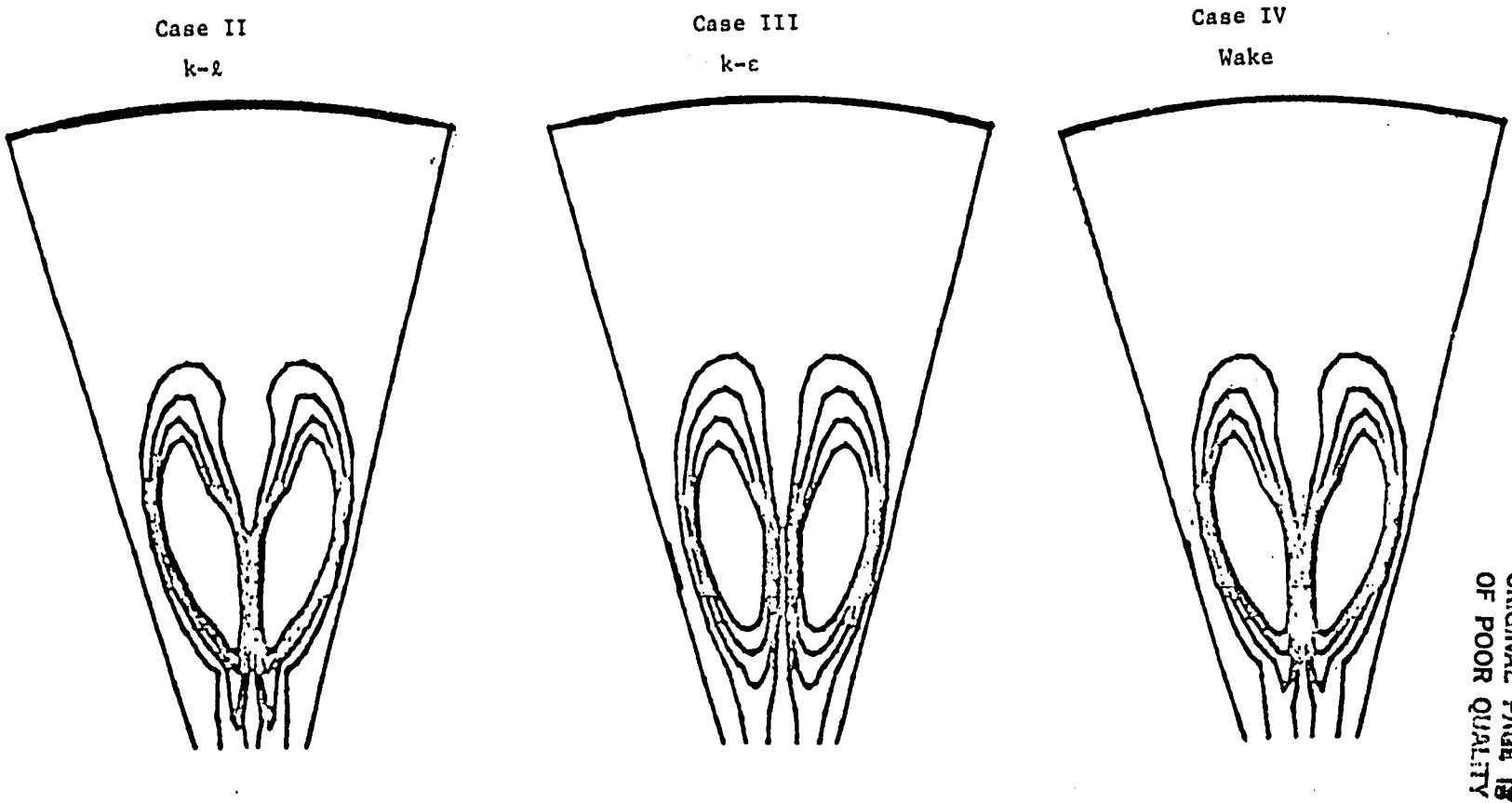

Fig. 7 - Effect of turbulence model on exit plane secondary flow vorticity contours.

Fig. 8 - Effect of swirl on exit plane total temperature contours.

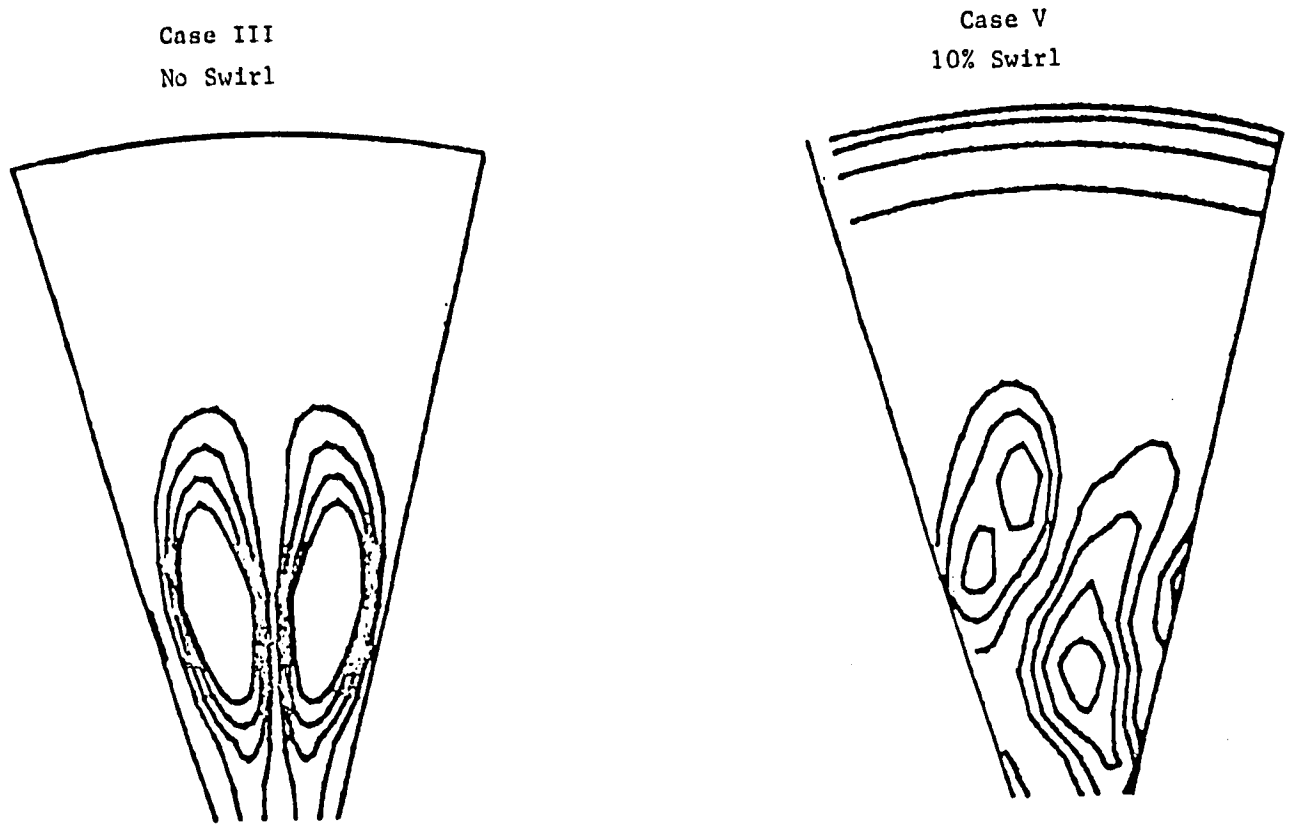

Fig. 9 - Effect of swirl on exit plane secondary flow vorticity contours.

Case VI

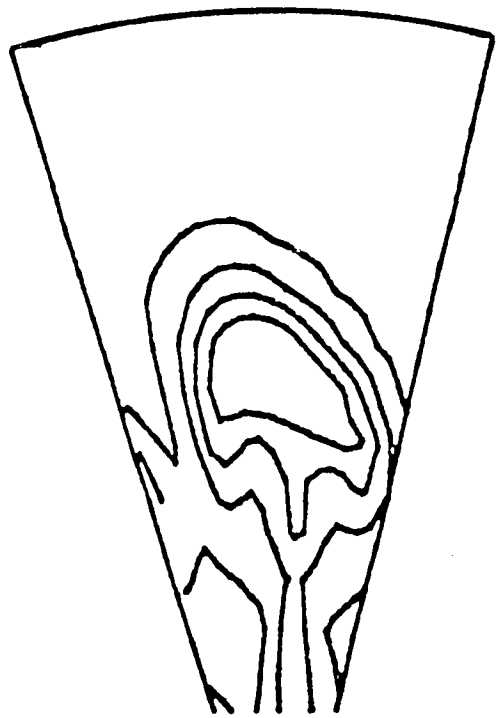

Fig. 10 - Distortion of exit plane total temperature contour with 10% swirl confined to outer half of mixing duct.

APPENDIX - USER'S GUIDE

Introduction

The Mixer computer code may be run using initial conditions obtained from experimental data and read in on a pointwise basis, or an initial flow field may be generated by the code itself upon parametric specification of the proper input variables. In either case, the originally specified flow fields are processed by the code to assure that the initial flow field is consistent with the finite-difference approximations to the governing equations. When parametric specification of initial conditions is used, it is also possible to activate a swirling flow option of the code. When this option is utilized the flow is assumed to be periodic, and the initial conditions, with the exception of the swirl velocity, are assumed to be symmetrical about the lobe centerline. Calculations performed with swirl must, therefore, consider a full lobe within the computational transverse planes, whereas only a half lobe need be considered for nonswirling flows.

In an effort to keep the initial condition specification similar for both swirling and nonswirling flow calculations, the initial flow field for swirling flow, or other calculations performed using periodic boundary conditions, is set up for half the lobe and then reflected. As a result, the user may use the same input run stream for both periodic and nonperiodic calculations by adjusting only the number of grid points, the aximuthal computational limits, and calling for the proper options. Specification of the lobe shape need not be altered; only half a lobe must be specified via the input in either case.

The user should read over all input descriptions before attempting to set up a case.

DESCRIPTION OF INPUT

Input to the MIXER code is accomplished by a combination of card input and information which is stored on auxiliary files. Metric information generated by the ADD code [13] and restart data sets are stored on separate auxiliary files. Program control is performed through card input, which is divided into three categories:

1) Plot file information for NASA-Lewis plotting package,
2) NAMELIST input, and
3) Experimental flow field input.

Format of the required input is as follows:

Plot File Input

CARD #	COLUMNS	VARIABLE	DESCRIPTION
Card 1	Col. 1-32	TITLE(I)	Plot title, format 5A6,A2. (May be left blank).
Card 2	Col. 1-2	ISYM	Twice the number of lobes in a 360^{o} cross section of the mixer geometry.
	Col. 3-12	SYSTEM	Indicates the type of coordinate system for plot routines. Format F10.0, Use SYSTEM=2.

NAMELIST IN1

Namelist	Description
$IN1	
RG	Gas constant, ft lb_f/(slug ^oR), default 1716.3 (air).
CP	Constant pressure specific heat, ft lb_f/(slug ^oR), default is 6012.384 (air).
TZERO	Reference temperature, assumed to be nominal primary stream temperature in degrees Rankine.
UZERO	Reference velocity, assumed to be nominal primary stream velocity, ft/sec.
PZERO1	Reference static pressure, assumed to be nominal pressure at initial plane, lb_f/ft^2, default is 2116.8.
YZERO	Reference length, ft.
VISC1	Reference viscosity, slugs/ft-sec.
$END	

NAMELIST IN2

The desired computational options and mesh information are specified in namelist $IN2.

Namelist	Description
$IN2	
IAXI	=1, cylindrical coordinates.
	=2, rotated orthogonal coordinates generated from ADD code geometry file. Default.
	If IAXI is input = 2 (or defaulted) the variables, XENTR, ILAP, LX, LY, and IPCOR must also be input.
XENTR	Dimensionless distance from initial ADD code potential line to initial plane of lobe mixer calculation. Used only for IAXI=2. Determined from ADD code parameters as XENTR=($JSTEP_{XENTR}$-1)*DS where $JSTEP_{XENTR}$ is the number of the ADD code potential surface representing the MIXER code initial plane and DS is the streamwise delta used in the ADD code. See Fig. B1.

Namelist	Description
ILAP	= 1 for IAXI=2 = 0 if IAXI=1 ILAP is defaulted = 1. If IAXI is set to 1, ILAP must be specified as 0.
LX	LX is the number of potential lines in the ADD code geometry file. LX must be input if ILAP=1.
LY	LY is the number of streamlines in the ADD code geometry file. LY must be input if ILAP=1.
IPCOR	IPCOR is used with ILAP=1 to identify the potential surface whose average dimensionless velocity is 1.0 in the axisymmetric potential calculation. IPCOR should be input as IPCOR=$JSTEP_{XENTR}$ in general.
ICOMP	= -1, stop after input dump. = 0, normal run (default). = 1, stop after printing initial plane geometry. = 2, stop after printing initial flow field.
IDATA	= 0, automated start (default). = 2, read initial velocity and temperature field data at each grid point.
ILAM	ILAM=1, Laminar flow. ILAM=0, k-ε turbulence model. ILAM=-1, Wake turbulence model. ILAM=-3, k-ℓ turbulence model.
IDIS	=1, specify uniform turbulence kinetic energy, at the turbine stream value throughout the initial flow field. =0, initial turbulence kinetic energy assumes turbulence production equal to dissipation. IDIS=1 is recommended.
LOWRE	=0, use high Reynolds number form of turbulence model equations =1, use low Reynolds number turbulence model equations. Requires IDIS=0, ILAM=0 or -3, and proper specification of wall boundary layers. Also requires a high degree of resolution of near wall regions using IGRID(I)=1 or 2 option with appropriate EPS(I). This option is not generally recommended for mixer flows.

Namelist	Description
YS(I,J)	YS(I,J) sets the limits of the transverse computational planes. YS(1,1) = r_{min} (dimensionless, r/YZERO) YS(2,1) = r_{max} (dimensionless, r/YZERO) YS(1,2) = θ_{min} (radians) YS(2,2) = θ_{max} (radians) For mixer geometries generated by the ADD code YS(1,1) must be the dimensionless plug radius at the first ADD code station RMIN, and Y(2,1) must be 1.0. See Fig. B-1. For non-swirling or non-periodic flows, YS(1,2) must correspond to the θ value at the maximum lobe penetration and YS(2,2) to the θ value midway between the lobes. See Fig. B-2. For periodic or swirling flows, YS(2,1) and YS(2,2) correspond to sequential values of θ midway between the lobes. See Fig. B-3.
NE(I)	NE(1) = number of grid points in the radial direction. NE(2) = number of azimuthal grid points. For periodic calculation NE(2) must be odd. Maximum values for NE(I) are 50. For periodic calculation NE(2)max = 49.
IGRID(I)	IGRID=0, no grid stretching (default). =1, Roberts stretching at r_{min} or θ_{min}. =2, Roberts stretching at both r_{min} and r_{max} or θ_{min} and θ_{max}. =4, hyperbolic sine stretch about XCTR(I). I=1 for radial direction, I=2 for aximuthal direction.
EPS(I)	Used for IGRID(I)≠0 to control the grid stretch near boundaries. For Roberts stretching 0.0 < EPS < 1.0. For hyperbolic sine 1.0 < EPS < 5.0.
XCTR(I)	Used only with IGRID(I)=4 to specify the r(I=1) or θ(I=2) location about which grid points are clustered. YS(1,I) < XCTR(I) < YS(2,I).
NS	Number of axial stations to be computed. NS=1 is initial plane. Maximum value is 50.
AP	If AP is input .GT.0 a geometric streamwise grid is set up with Δx(J)/Δx(J-1) = AP. If AP is input .LT.0 the user must specify the axial mesh. AP has a default of 1.05 but the AP.LT.0 option is recommended.

X(JX)	X is an array which contains NS values of the streamwise mesh coordinate. If AP is input .GT.0 only X(1) and X(2) need be input. If AP is input .LT.0 NS values of X must be input. If IAXI=1, X is a physical but dimensionless distance. If IAXI=2 and ADD code geometry is used, X represents the dimensionless computational distance from the initial plane. The maximum allowable value of X is given as $(JSTEP_{MAX} - JSTEP_{XENTR})*DS/USCALE$ where USCALE=YS(2,1)/(YS(2,1)-YS(1,1)). The maximum value of X should be slightly less than this value to avoid marching out of the ADD code geometry which will result in an error termination. See Fig. B1.
IPERIO	=0, normal calculation =1, periodic option activated. Input must be set up for periodic flow field. Check NE(2) specification.
ISWIRL	=0, nonswirling flow. =1, swirling flow. Requires IPERIO=1. Also requires values for RSW1, RSW2, VSWRL, and DELSWL.
$END	

NAMELIST IN3

Restart and plot file information is specified in namelist $IN3.

Namelist	Description
$IN3	
IRSTIN	The number of the axial station to be read in for a restart. No restart if IRSTIN=0 (default).
IRSTOT	Increment for saving restart information. Restart files will be written every IRSTOT steps from starting value of JX, the axial station counter. Default assumes no restarts written. On a restart, the starting value of JX = IRSTIN.
JRSTIN	File number from which restart information is to be read. Default file number is 11.
JRSTOT	File number onto which restart information is to be written. Default file number is 11.

Namelist	Description
NFILE	Sequence number in file JRSTIN of the desired restart information.
NSAVED	The number of restart data blocks saved on file JRSTOT.
IPLOT	If IPLOT≥1 a plot file must be assigned in the run stream and information will be written in this file for subsequent use in plotting. IPLOT=0 gives no plot file. Default is IPLOT=0. A plot file will be written every IPLOT th station.

$END

NAMELIST IN4

Velocity and temperature ratios between the two streams are specified in namelist $IN4, as are turbulence levels and information used to construct the initial secondary flows.

Namelist	Description
$IN4	
USTRM2	Ratio of secondary stream (fan) velocity to primary stream (turbine) velocity. For matched average inlet Mach numbers and total pressures USTRM2= $\sqrt{TSTRM2}$. Default value is USTRM2=.707.
TSTRM2	Ratio of secondary stream temperature to primary stream temperature. Default is TSTRM2=.5.
TUSTR1	Primary stream turbulence intensity. $T_{u1}= \overline{u'^2}/u_1^2$ where u_1=UZERO.
TUSTR2	Secondary stream turbulence intensity. $T_{u2}= \overline{u'^2}/u_2^2$ where u_2=UZEROxUSTRM2. If TUSTR2 is input as 0.0 the free stream turbulence in both streams ($k=3T_u^2/2$) is assumed equal to $3T_{u1}^2/2$. If IDIS=1 is input (as recommended) only TUSTR1 is used.
ALEN	Dimensionless free stream turbulent length scale, ℓref/YZERO. To be estimated by the user based on geometric constraints of the mixing duct and boundary layers. ALEN should be on the order of .1 of estimated free shear layer or boundary layer thickness.
AMEXIT	AMEXIT is an assumed exit plane Mach number which is used to specify the isentropic exit plane pressure for the thrust calculation. Default value is AMEXIT=0.9.

Namelist	Description
DELMIX	DELMIX is input with IDATA .GT. 0 as a dimensionless boundary layer thickness presumed to be representative of the boundary layers on the lobe surfaces. It is used in computing the initial turbulence length scale.
DELHUB	DELHUB is input with IDATA .GT. 0 as a dimensionless boundary layer thickness, δ/YZERO, respresentative of the hub boundary layer. It is used in computing the initial turbulence length scale. See IHUB in $IN5.
DELSHR	Similar to DELHUB but pertaining to the shroud boundary layer. See ISHR in $IN5.
RHUB	RHUB is a dimensionaless secondary flow hub boundary layer thickness used to construct initial secondary flow profiles required for IDATA=0 or 2.
RTIP	Similar to RHUB but pertaining to the shroud secondary flow boundary layer.
DELSEC	DELSEC is a dimensionless secondary flow boundary layer thickness used to construct the initial vorticity profile. A value on the order of (RTIP+RHUB)/2 should be used.
VFAN	Used with IDATA=0. VFAN is the ratio of the local radial velocity to the local streamwise velocity (positive outward) in the fan stream.
VCORE	Used with IDATA=0. VCORE is the ratio of the local radial velocity to the local streamwise velocity (positive outward) in the turbine stream.
VSWRL	VSWRL is used only with ISWIRL=1 to specify the dimensionless swirl velocity magnitude.
RSW1, RSW2	RSW1 and RSW2 are the radial limits over which swirl velocity is to be specified. They must be input such that YS(1,1) < RSW1 < RSW2< YS(2,1).
DELSWL	DELSWL is a dimensionless length scale over which the swirl velocity in increased from zero to its' maximum value. DELSWL must be less than (RSW2 - RSW1)/2.

$END

NAMELIST IN5

The lobe shape and primary flow boundary layer parameters are specified in namelist $IN5. Specification of this information should be performed using Fig. B2 or B3 as a guide.

Namelist	Description
$IN5	
ILOBE	ILOBE is a flag used in the automated starting routine. ILOBE=0 indicates that no boundary layers are to be set up on the lobe surfaces. ILOBE=2 indicates that lobe boundary layers are to be set up.

Namelist	Description
IHUB	IHUB=0 indicates that hub boundary layers will not be present in the initial profile, regardless of other starting options. If IDATA is input .GT.0 and IHUB is input .GT.0 DELHUB must be input. If the IDATA option is not used, and hub boundary layers are desired, IHUB must be input equal to the number of points input to describe the hub boundary layer in the array BLHUB.
ISHR	ISHR is similar to IHUB except it pertains to the shroud boundary layer.
BLHUB(I,J)	If hub and/or shroud boundary layers are to be constructed using the automated starting routine (IDATA=0) the boundary layer displacement thickness and shape factor must be input as functions of θ along the hub and/or shroud surfaces. This is accomplished using the array BLHUB. See Fig. B2. BLHUB(I,1) contains the values of θ (in radians) where hub boundary layer parameters are specified. The θ values are arbitrary but they must increase monotonically. For calculation using the IPERIO=0 option the first value must be slightly less than θ_{min} and the last value must be slightly greater than θ_{max}. For IPERIO=1, the first θ value must be slightly less than that of $(\theta_{min} + \theta_{max})/2$. A maximum of 20 values may be specified. The number of θ values specified must be equal to the input value of IHUB. BLHUB(I,2)=θ^*/YZERO, the dimensionless displacement thickness of the hub boundary layer at each specified θ location. BLHUB(I,3)=H, the shape factor at each θ location. BLHUB(I,4) is the shroud equivalent of BLHUB(I,1). ISHR values of θ must be loaded in BLHUB(I,4). BLHUB(I,5) and BLHUB(I,6) are similar to BLHUB(I,2) and BLHUB(I,3) except they pertain to the shroud boundary layer parameters.
NLOBE	NLOBE is the number of data points input to describe the lobe shape and lobe boundary layers.
YLOBE(I,J)	YLOBE is an array which contains the data needed to specify the lobe shape and boundary layers which may be on each side of the lobe surface. NLOBE values of each parameter in YLOBE must be specified. See Fig. B2 for ordering of information. Specification of the lobe shape must start where the lobe crosses the θ_{max} boundary.

Namelist	Description
YLOBE(I,J)	YLOBE(I,1) contains NLOBE dimensionless radial coordinates, R/YZERO, of the lobe. The first point must be the radial coordinate where the lobe crosses the θ_{max} boundary. The last point must be the radial coordinate value where the lobe crosses the θ_{min} boundary for IPERIO=0. For IPERIO=1 only half the lobe shape is specified, thus the last point is the radial coordinate where $\theta = (\theta_{min} + \theta_{max})/2$. See Fig. B2. YLOBE(I,2) contains the θ values corresponding to the R values loaded in YLOBE(I,1). The first value (I=1) must be slightly greater than θ_{max}. For IPERIO=0 the last value (I=NLOBE) must be slightly less than θ_{min}. For IPERIO=1 the last value must be slightly less than $(\theta_{min} + \theta_{max})/2$. YLOBE(I,3) contains NLOBE values of the dimensionless displacement thickness, δ^*/YZERO, for the boundary layer on the turbine stream side of the lobe surface at the lobe coordinate locations specified in YLOBE(I,1) and YLOBE(I,2). YLOBE(I,4) is the same as YLOBE(I,3) except it pertains to the fan stream side of the lobe. YLOBE(I,5) contains the distribution of the shape factors, H, at each coordinate point for the turbine stream side of the lobe. Finally, YLOBE(I,6) contains the shape factor distribution for the fan stream side. YLOBE(I,3) through YLOBE(I,6) need not be specified if the IDATA option is specified, or if ILOBE=0. YLOBE(I,1) and YLOBE(I,2), the r-θ coordinates of the lobe, must be specified for all starting options.
IWAKE	If IWAKE=1 the slots for shape factor in BLHUB and YLOBE need not be input as a value of the wake function in the boundary layer profile is assumed.
$END	

When setting up a lobe shape it is advantageous to consider specification of BLHUB and YLOBE for a <u>non periodic</u> calculation (IPERIO=0). Under these conditions the computation segment appears as in Fig. B2. If θ_{min} is specified as zero, and θ_{max} is specified as positive, and the lobe shape is properly specified, then a periodic calculation can be performed <u>without</u> changing the YLOBE or BLHUB arrays simply by setting $\theta_{min} = -\theta_{max}$, adjusting the number of

θ grid points, and by specifying IPERIO=1. In general, if the arrays YLOBE and BLHUB are properly specified for a nonperiodic calculation of limits θ_{min} to θ_{max}, the same lobe shape specification will be correct for periodic calculations in which θ_{max} remains unchanged, and θ_{min} is reset as $\theta_{min}=2\theta_{min}-\theta_{max}$.

NAMELIST IN6

Boundary conditions are specified in namelist IN6. For periodic flows θ direction boundary conditions are ignored. The boundary conditions are set to defaults appropriate for mixer calculations performed with wall functions. Only XCBC must be specified.

Namelist	Description
$IN6	
NBCON(I,J,K)	NBCON is a three-dimensional array which allows the user to select the desired boundary conditions for the primary flow momentum equation, the energy equation, the secondary flow stream function-vorticity system, and the turbulence model equations. The subscript "J" determines the boundary surface. J=1 for the surface at R_{min}, J=2 for R_{max}, J=3 for θ_{min}, J=4 for θ_{max}.
NBCON(1,J,1)	NBCON(1,J,1) is used to specify boundary condition for the primary flow momentum equation. = 0 - no slip = 1 - zero normal gradient = 2 - zero second derivative = 4 - wall function At the hub (J=1) and shroud (J=2) either no slip or wall functions should be specified. (Wall functions are preferred, and required when LOWRE=0 in $IN2). At θ_{min} (J=3) and θ_{max} (J=4) symmetry (zero gradient) conditions are required when IPERIO=0.
NBCON(2,J,1)	NBCON (2,J,1) is used for the energy equation. = 1 - zero normal gradient (adiabatic) = 2 - zero second derivative. Adiabatic conditions should be specified at all surfaces (J=1 to 4).
NBCON(4,J,1)	NBCON(4,J,1) is used to specify boundary conditions for the vorticity-vector potential system, and results in either no slip or slip conditions applied to the local tangential component of the secondary flow velocity. = 0 - no slip = 1 - slip with zero vorticity

At r_{min} (J=1) and r_{max} (J=2) no slip should be specified. At θ_{min} (J=3) and θ_{max} (J=4) symmetry implies slip with zero vorticity should be specified. The no slip condition should be used at a centerline.

NBCON(1,J,2)

NBCON(1,J,2) is used to specify boundary conditions for the turbulence kinetic energy equation which is solved if ILAM=0 or -3.

= 0 - zero kinetic energy

= 1 - zero normal gradient

= 2 - zero second derivative

At r_{min} (J=1) and r_{max} (J=2) the turbulence kinetic energy should be set to zero if LOWRE=1, or the normal gradient should be set to zero if LOWRE=0. The latter is consistent with the wall functions used for the primary flow momentum, and is recommended. At θ_{min} (J=3) and θ_{max} (J=4) zero normal gradient should be specified.

NBCON(2,J,2)

NBCON(2,J,2) is used to specify boundary conditions for the turbulence dissipation equation (ILAM=0 only).

= 0 - zero dissipation

= 1 - zero normal gradient

= 2 - zero second derivative

= 4 - wall function type boundary condition

At r_{min} (J=1) and r_{max} (J=2) the dissipation should be set to zero if LOWRE=1, or the wall function should be used if LOWRE=0. The later is recommended. At θ_{min} and θ_{max} zero gradients should be applied.

XCBC

XCBC is used in MIXER calculations to change boundary conditions as the flow moves downstream off the hub, where wall function boundary conditions are applied, to a center line where symmetry conditions are applied. The user must specify the value of XCBC by examination of the geometry from the ADD code. XCBC is computed as XCBC=($JSTEP_{XCBC}$ - $JSTEP_{XENTR}$)*DS where $JSTEP_{XCBC}$ is the number of the ADD code potential line where the plug degenerates to a center line and $JSTEP_{XENTR}$ is the number of the potential line representing the initial MIXER calculation plane. See Fig. B1. The default value causes no changes.

NBCONC(I,J,K)

NBCONC has the same function as NBCON but is used to specify which boundary conditions are to be changed for X>XCBC and what they are to be. Default value will cause no change in boundary conditions regardless of the value of XCBC. For a calculation with hub boundary layer, NBCONC is used to change from wall functions to symmetry conditions as the hub degenerates to a center line.

$END

NAMELIST IN7

$IN7

IPRN(I)

IPRN is an array which selects variables to be printed at each axial station. If IPRN(I)=1 variable "I" will be printed. If IPRN(I)=0 variable "I" will not be printed. The variables are numbered as follows:

I=	Variable
1	u
2	v
3	w
4	ρ
5	E
6	μ_T
7	k
8	ε
9	ξ
10	ψ
11	M
12	static temperature ratio T/T_r
13	total temperature T^o/T^o_r
14	pressure coefficient
15	static pressure ratio P/P_r
16	total pressure ratio P^o/P^o_r
17	swirl angle, degrees
18	$\overline{u'v'}$
19	$\overline{u'w'}$
20	$\overline{v'w'}$

ICON

ICON controls printer contour plots of the printed flow field variable.

ICON=1 produces printer contour plots.

ICON=0, no contour plots.

IPRINT — IPRINT must be input ≥1. Printout will be made every IPRINT'th station.

$END

Experimental Flow Field Input

The following cards are needed only if starting profiles are to be read in (IDATA=2). Each card contains velocity components u, v, w in feet per second and static temperature, T, in degrees Rankine at each computational grid point. One card per grid point is required, thus a total of NE(1)*NE(2) data cards are needed. Format 4F10.0. The data is read for the grid point numbering shown in Fig. B4.

CARDS # $END+1 to $END+NE(1)*NE(2)

Col. 1-10 — u - velocity component in the computational streamwise direction, ft/sec.

11-20 — v - velocity component in the computational radial direction, ft/sec.

21-30 — w - velocity component in the computational azimuthal direction, ft/sec.

31-40 — T - static temperature, ^{o}R.

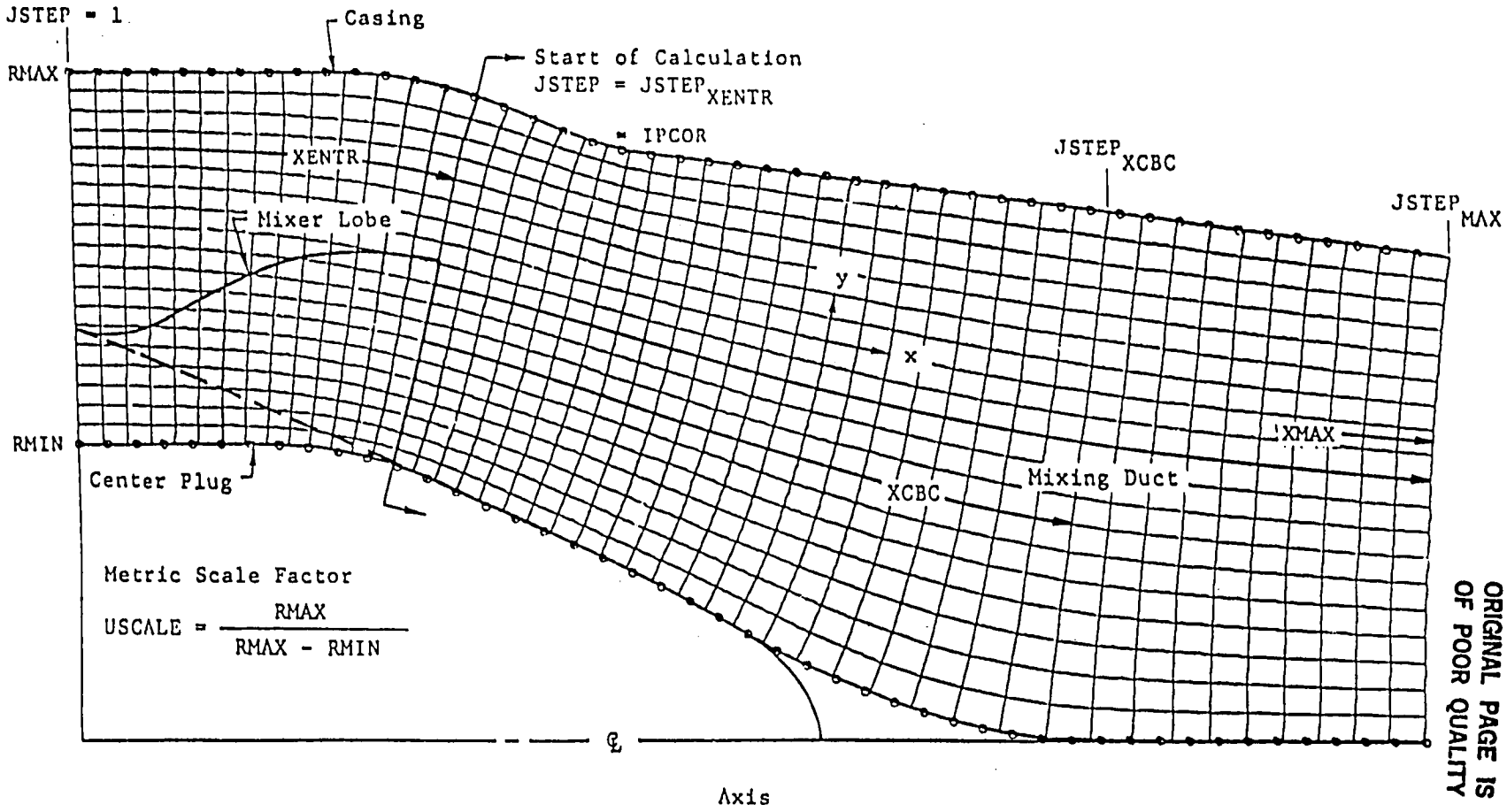

Figure B1. - Typical coordinate system and definition of input parameters.

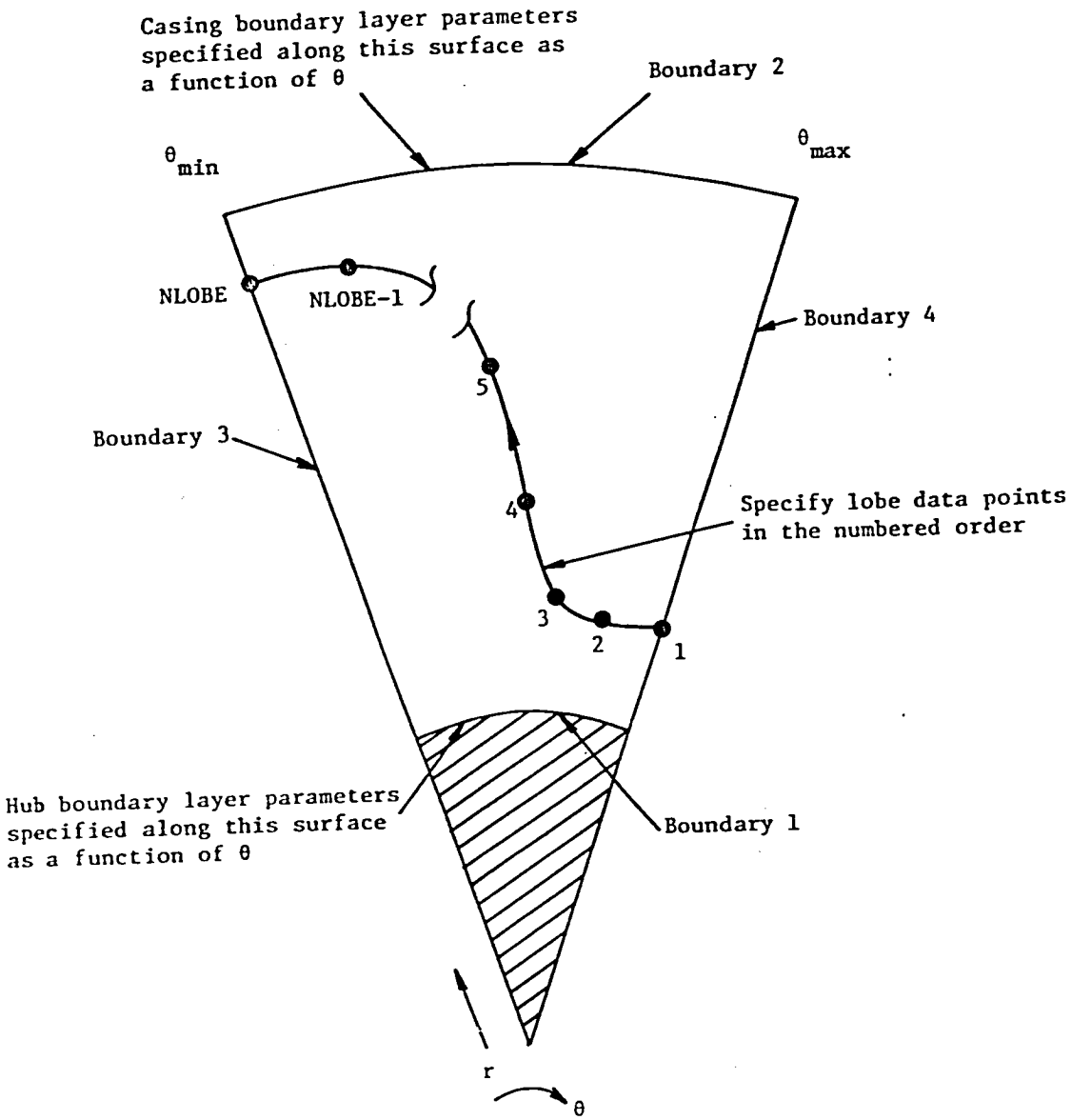

Figure B2. - Specification of the lobe shape and hub and casing boundary layers.

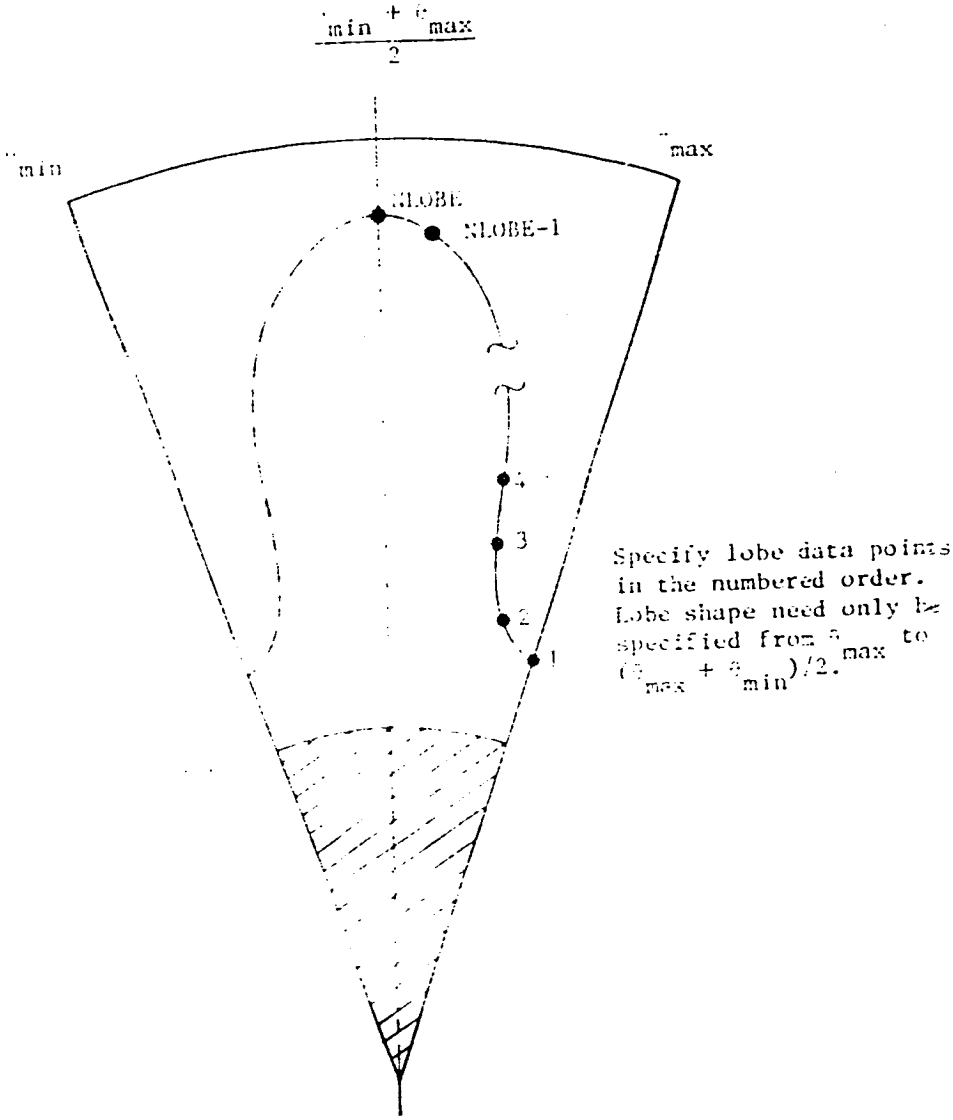

Figure B3. - Specification of lobe shape for periodic flow domain.

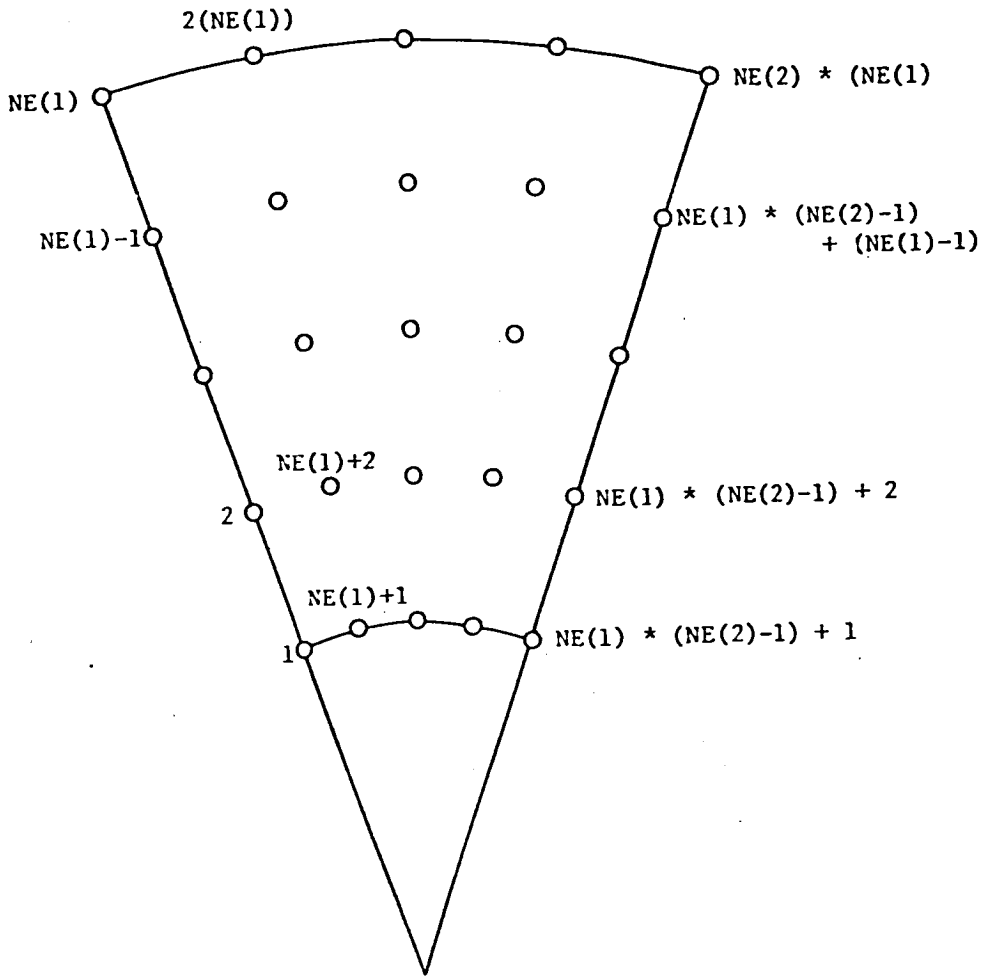

Figure B4. - Ordering of grid points for IDATA option.

END

DATE

FILMED

FEB 23 1984